

# Application of reduced Rayleigh equations to electromagnetic wave scattering by two-dimensional randomly rough surfaces

Antoine Soubret,<sup>1,2,\*</sup> Gérard Berginc,<sup>1</sup> and Claude Bourely<sup>2</sup>

<sup>1</sup>Thomson-CSF Optronique, Boîte Postale 55, 78233 Guyancourt Cedex, France

<sup>2</sup>Centre de Physique Théorique, CNRS-Luminy Case 907, 13288 Marseille Cedex 9, France

(Received 22 September 2000; published 5 June 2001)

The small perturbation method has been extensively used for wave scattering by rough surfaces. The standard method developed by Rice is difficult to apply when we consider second and third orders of scattered fields as functions of the surface height. Calculations can be greatly simplified with the use of reduced Rayleigh equations, because one of the unknown fields can be eliminated. We derive a set of four reduced equations for the scattering amplitudes, which are applied to cases of a rough conducting surface, and to a slab where one of the boundaries is a rough surface. As in the one-dimensional case, numerical simulations show the appearance of enhanced backscattering for these structures.

DOI: 10.1103/PhysRevB.63.245411

PACS number(s): 42.25.Fx, 42.25.Ja, 42.25.Gy, 78.66.Bz

## I. INTRODUCTION

The scattering of electromagnetic waves from a rough surface has been studied in different domains such as radio-physics, geophysical remote sensing, ocean acoustics, and surface optics.<sup>1-11</sup> One of the earliest theories used is the small perturbation method (SPM) originally developed by Rice.<sup>12</sup> This theory still remains of interest,<sup>11,13,14</sup> because perturbative terms of orders higher than 1 can produce enhanced backscattering, or improve prediction accuracy in an emission model. Although the Rice method can be used in principle to determine all orders in the perturbative development, very few works use terms of order higher than 1 for a two-dimensional surface due to the calculational complexity. The second order was written in a compact form by Voronovich<sup>15</sup> in his work on the small-slope approximation, and only recently was the third order presented.<sup>13</sup> However, there exists a different way to obtain the SPM which dates back from the work of Brown *et al.*<sup>16</sup> Using both the Rayleigh hypothesis and the extinction theorem, they obtained an integral equation, called the reduced Rayleigh equation, which involves only the incident and scattered fields alone. In their method the field transmitted through the surface is eliminated in such a way that the scattered field becomes a function of the incident field only. This reduced equation was extensively used by Maradudin and co-workers to study localization effects by a conducting surface,<sup>17-19</sup> coherent effects in reflection factor,<sup>20</sup> and scattering by one-dimensional<sup>21</sup> and two-dimensional conducting surface.<sup>22</sup> It should be noted that the third-order perturbation term was already explicated in the work of Ref. 22.

In recent years, similar studies were made in the case of thin films bounded by a rough surface,<sup>11,23</sup> but only in the one-dimensional case.<sup>24</sup> In order to calculate the two-dimensional case it becomes necessary to derive an extension of the reduced Rayleigh equation for this system. In the present paper, we first study a surface where down- and up-going fields exist both on the upper and lower sides of the film. We show the existence of four equations, that we also call reduced Rayleigh equations, which have the property

that one of the down- or up-going fields is eliminated. With these equations, we rediscover the equation obtained by Brown *et al.*<sup>16</sup> for one rough surface, and derive the corresponding ones for a slab where one of the boundaries is a rough surface. Next a perturbative development, up to third order, is obtained in a compact matrix form for these two systems. This third-order term is mandatory if we need an expression for the cross section up to the fourth-order approximation. As in the one-dimensional case, the results of the incoherent cross section show a well-defined peak in the retroreflection direction.

In the case of small-roughness metallic surfaces, this peak was originally explained by the infinite perturbation theory,<sup>17-19</sup> and further developments<sup>21</sup> showed that the major contribution to the enhanced backscattering peak comes from the second-order term in the field perturbation. However, in the one-dimensional case the enhanced backscattering for a rough surface, appears only for a (TM) incident wave due to the fact that plasmon polaritons only exist for this polarization. In the two-dimensional case, due to the existence of cross polarization, we will show that an incident TE wave can excite a TM plasmon mode which can transform into a TE or TM volume electromagnetic wave. Thus the enhanced backscattering is present independently of the polarization of the incident and scattered waves. For a rough dielectric film bounded by a conducting plane, enhanced backscattering is present for both TE and TM incident waves, even in the one-dimensional case, because guided waves exist for these two polarizations. The qualitative effect of the two-dimensional surface is particularly sensitive when we study thin films. For instance, in the one-dimensional case, satellite peaks<sup>11,23</sup> appear on each side of the enhanced backscattering peaks; however, in the two-dimensional case, the coupling between TE and TM modes drastically attenuates these peaks.

The paper is organized as follows. In Sec. II, we derive the four reduced Rayleigh equations. In Sec. III, we introduce the diffusion matrix. In Sec. IV, we determine the perturbative development up to the third-order term in the surface height, for a rough surface alone, and for slab with a rough surface located at one of the boundaries. In Sec. V, we

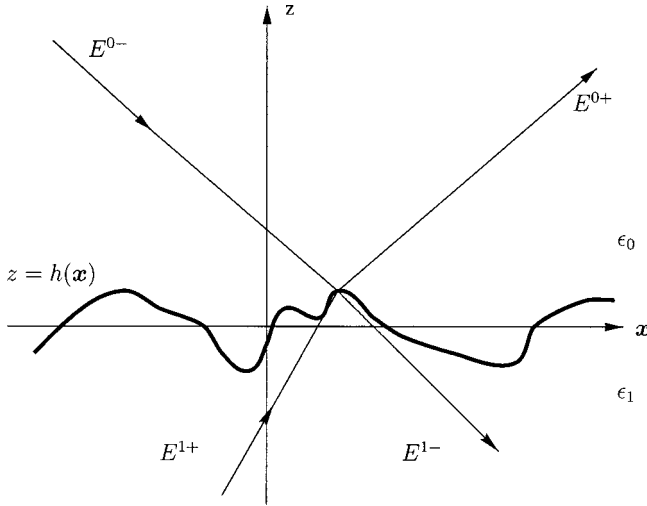


FIG. 1. A rough surface with an incident wave coming from both sides of media 0 and 1.

introduce the Mueller matrix, and the definition of the statistical parameters for the rough surface. We then obtain the bistatic matrix in terms of a perturbative development. Numerical examples which show the enhanced backscattering are presented in Sec. VI. Conclusions drawn from the results of our calculations, are discussed in Sec. VII.

## II. DERIVATION OF THE REDUCED RAYLEIGH EQUATION

The reduced Rayleigh equation was obtained for a two-dimensional surface by Brown *et al.*<sup>16</sup> using the extinction theorem and the Rayleigh hypothesis. It allows one to calculate the scattered field from the rough surface. Now, if we want to compute the transmitted field from a rough surface, we have to introduce another reduced Rayleigh equation derived by Greffet.<sup>25</sup> However, these two equations were established in the case where there is no up-going field inside the medium; thus they cannot be used to obtain the field scattered by a slab with a rough surface on its upper side. In fact, to generalize these equations to a slab, we have to consider all the fields shown in Fig. 1. We will prove that there exist four reduced Rayleigh equations, which involve only three of the participating fields  $\mathbf{E}^{0-}$ ,  $\mathbf{E}^{0+}$ ,  $\mathbf{E}^{1-}$ , and  $\mathbf{E}^{1+}$ .

We consider that each electromagnetic wave propagates with a frequency  $\omega$ , and in the following the factor  $\exp(-i\omega t)$  will be omitted. We choose to work with a Cartesian coordinate system  $\mathbf{r}=(\mathbf{x},z)=(x,y,z)$ , where the  $z$  axis is directed upward, and we consider a boundary of the form  $z=h(\mathbf{x})$ . Moreover, we suppose that there exists a length  $L$  for which  $h(x,y)=0$ , if  $|x|\geq L/2$  or  $|y|\geq L/2$ , and  $L$  may be arbitrarily large but finite.

### A. Propagation equations and boundary conditions

The electric field  $\mathbf{E}$  satisfies the Helmholtz equation in the two media:

$$(\nabla^2 + \epsilon_0 K_0^2)\mathbf{E}^0(\mathbf{r})=0 \quad \text{for } z>h(\mathbf{x}), \quad (1)$$

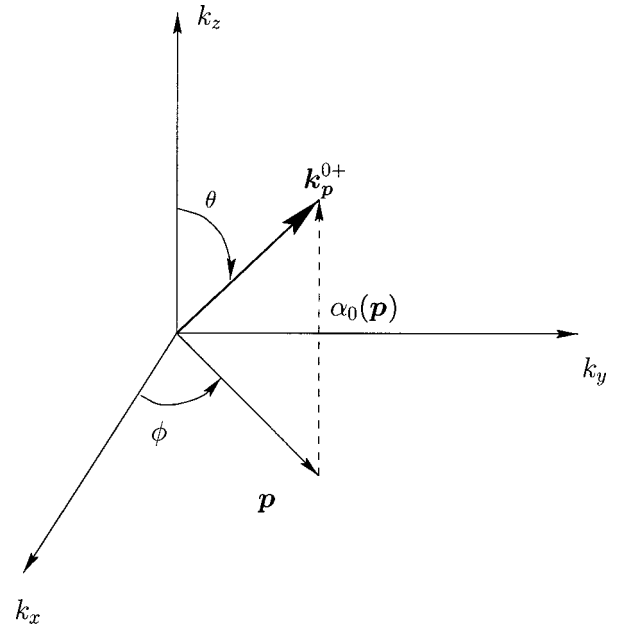


FIG. 2. Decomposition of the wave vector  $\mathbf{k}^{0+}$ .

$$(\nabla^2 + \epsilon_1 K_0^2)\mathbf{E}^1(\mathbf{r})=0 \quad \text{for } z<h(\mathbf{x}), \quad (2)$$

where  $K_0=\omega/c$ . Since the system is homogeneous in the  $\mathbf{x}=(x,y)$  directions, we can represent the electric field by its Fourier transform. Thus, using the Helmholtz equation, we deduce the following expression for the electric field<sup>8,10</sup> in the medium 0:

$$\begin{aligned} \mathbf{E}^0(\mathbf{r}) = & \int \frac{d^2\mathbf{p}}{(2\pi)^2} \mathbf{E}^{0-}(\mathbf{p}) \exp(i\mathbf{k}_p^{0-} \cdot \mathbf{r}) \\ & + \int \frac{d^2\mathbf{p}}{(2\pi)^2} \mathbf{E}^{0+}(\mathbf{p}) \exp(i\mathbf{k}_p^{0+} \cdot \mathbf{r}), \end{aligned} \quad (3)$$

where (see Fig. 2)

$$\alpha_0(\mathbf{p}) \equiv (\epsilon_0 K_0^2 - \mathbf{p}^2)^{1/2}, \quad (4)$$

$$\mathbf{k}_p^{0\pm} \equiv \mathbf{p} \pm \alpha_0(\mathbf{p}) \hat{\mathbf{e}}_z. \quad (5)$$

In fact, when writing such a definition, we implicitly make the assumption that the Rayleigh hypothesis is correct. This representation is only valid when  $z>\max[h(\mathbf{x})]$ , and in this case  $\mathbf{E}^{0-}(\mathbf{p})$  represents the incident wave amplitude. In order to be correct we need to add an explicit dependence in the  $z$  coordinate like (see Ref. 26):

$$\mathbf{E}^{0-} = \mathbf{E}^{0-}(\mathbf{p}, z), \quad \mathbf{E}^{0+} = \mathbf{E}^{0+}(\mathbf{p}, z). \quad (6)$$

However, explicit calculations in the case of infinite conducting surfaces,<sup>27</sup> and for a dielectric medium<sup>4</sup> without this hypothesis, have shown that the perturbative developments are identical. The validity of this hypothesis is no doubt a matter of the convergence domain, as discussed by Voronovich.<sup>8,15</sup>

In medium 1, we have a similar expression,

$$\begin{aligned} \mathbf{E}^1(\mathbf{r}) = & \int \frac{d^2\mathbf{p}}{(2\pi)^2} \mathbf{E}^{1-}(\mathbf{p}) \exp(i\mathbf{k}_p^{1-} \cdot \mathbf{r}) \\ & + \int \frac{d^2\mathbf{p}}{(2\pi)^2} \mathbf{E}^{1+}(\mathbf{p}) \exp(i\mathbf{k}_p^{1+} \cdot \mathbf{r}), \end{aligned} \quad (7)$$

where

$$\alpha_1(\mathbf{p}) \equiv (\epsilon_1 K_0^2 - \mathbf{p}^2)^{1/2}, \quad (8)$$

$$\mathbf{k}_p^{1\pm} \equiv \mathbf{p} \pm \alpha_1(\mathbf{p}) \hat{\mathbf{e}}_z. \quad (9)$$

We decompose the vectors  $\mathbf{E}(\mathbf{p})$  on a two-dimensional basis due to the fact that  $\nabla \cdot \mathbf{E}(\mathbf{r}) = 0$ , which gives the conditions

$$\mathbf{k}_p^{0\pm} \cdot \mathbf{E}^{0\pm}(\mathbf{p}) = 0, \quad \mathbf{k}_p^{1\pm} \cdot \mathbf{E}^{1\pm}(\mathbf{p}) = 0. \quad (10)$$

Then, we define the horizontal polarization vectors  $H$  for TE and  $V$  for TM in medium 0 by

$$\hat{\mathbf{e}}_H(\mathbf{p}) \equiv \frac{\hat{\mathbf{e}}_z \times \mathbf{k}_p^{0\pm}}{\|\hat{\mathbf{e}}_z \times \mathbf{k}_p^{0\pm}\|} = \hat{\mathbf{e}}_z \times \hat{\mathbf{p}}, \quad (11)$$

$$\hat{\mathbf{e}}_V^{0\pm}(\mathbf{p}) \equiv \frac{\hat{\mathbf{e}}_H(\mathbf{p}) \times \mathbf{k}_p^{0\pm}}{\|\hat{\mathbf{e}}_H(\mathbf{p}) \times \mathbf{k}_p^{0\pm}\|} = \pm \frac{\alpha_0(\mathbf{p})}{\sqrt{\epsilon_0} K_0} \hat{\mathbf{p}} - \frac{\|\mathbf{p}\|}{\sqrt{\epsilon_0} K_0} \hat{\mathbf{e}}_z, \quad (12)$$

with similar expressions for medium 1:

$$\hat{\mathbf{e}}_H(\mathbf{p}) \equiv \frac{\hat{\mathbf{e}}_z \times \mathbf{k}_p^{1\pm}}{\|\hat{\mathbf{e}}_z \times \mathbf{k}_p^{1\pm}\|} = \hat{\mathbf{e}}_z \times \hat{\mathbf{p}}, \quad (13)$$

$$\hat{\mathbf{e}}_V^{1\pm}(\mathbf{p}) \equiv \frac{\hat{\mathbf{e}}_H(\mathbf{p}) \times \mathbf{k}_p^{1\pm}}{\|\hat{\mathbf{e}}_H(\mathbf{p}) \times \mathbf{k}_p^{1\pm}\|} = \pm \frac{\alpha_1(\mathbf{p})}{\sqrt{\epsilon_1} K_0} \hat{\mathbf{p}} - \frac{\|\mathbf{p}\|}{\sqrt{\epsilon_1} K_0} \hat{\mathbf{e}}_z. \quad (14)$$

Thus we decompose the waves in medium 0 on the basis  $[\mathbf{p}]^{0-} \equiv [\hat{\mathbf{e}}_V^{0-}(\mathbf{p}), \hat{\mathbf{e}}_H(\mathbf{p})]$ , and  $[\mathbf{p}]^{0+} \equiv [\hat{\mathbf{e}}_V^{0+}(\mathbf{p}), \hat{\mathbf{e}}_H(\mathbf{p})]$ :

$$\mathbf{E}^{0-}(\mathbf{p}) = \begin{pmatrix} E_V^{0-}(\mathbf{p}) \\ E_H^{0-}(\mathbf{p}) \end{pmatrix}_{[\mathbf{p}]^{0-}}, \quad \mathbf{E}^{0+}(\mathbf{p}) = \begin{pmatrix} E_V^{0+}(\mathbf{p}) \\ E_H^{0+}(\mathbf{p}) \end{pmatrix}_{[\mathbf{p}]^{0+}}, \quad (15)$$

where for medium 1 on the basis  $[\mathbf{p}]^{1-} \equiv [\hat{\mathbf{e}}_V^{1-}(\mathbf{p}), \hat{\mathbf{e}}_H(\mathbf{p})]$  and  $[\mathbf{p}]^{1+} \equiv [\hat{\mathbf{e}}_V^{1+}(\mathbf{p}), \hat{\mathbf{e}}_H(\mathbf{p})]$

$$\mathbf{E}^{1-}(\mathbf{p}) = \begin{pmatrix} E_V^{1-}(\mathbf{p}) \\ E_H^{1-}(\mathbf{p}) \end{pmatrix}_{[\mathbf{p}]^{1-}}, \quad \mathbf{E}^{1+}(\mathbf{p}) = \begin{pmatrix} E_V^{1+}(\mathbf{p}) \\ E_H^{1+}(\mathbf{p}) \end{pmatrix}_{[\mathbf{p}]^{1+}}. \quad (16)$$

The electric field  $\mathbf{E}(\mathbf{x}, z)$  and magnetic field  $\mathbf{B}(\mathbf{x}, z) = (1/i\omega) \nabla \times \mathbf{E}(\mathbf{x}, z)$ , satisfy the following boundary conditions:

$$\mathbf{n}(\mathbf{x}) \times \{\mathbf{E}^0[\mathbf{x}, h(\mathbf{x})] - \mathbf{E}^1[\mathbf{x}, h(\mathbf{x})]\} = 0, \quad (17)$$

$$\mathbf{n}(\mathbf{x}) \cdot \{\epsilon_0 \mathbf{E}^0[\mathbf{x}, h(\mathbf{x})] - \epsilon_1 \mathbf{E}^1[\mathbf{x}, h(\mathbf{x})]\} = 0, \quad (18)$$

$$\mathbf{n}(\mathbf{x}) \times \{\mathbf{B}^0[\mathbf{x}, h(\mathbf{x})] - \mathbf{B}^1[\mathbf{x}, h(\mathbf{x})]\} = 0, \quad (19)$$

$$\mathbf{n}(\mathbf{x}) \equiv \hat{\mathbf{e}}_z - \nabla h(\mathbf{x}).$$

Let us introduce the fields Fourier transforms Eqs. (3) and (7), into the boundary conditions [Eqs. (17)–(19)], they give

$$\begin{aligned} & \sum_{a=\pm} \int \frac{d^2\mathbf{p}}{(2\pi)^2} \mathbf{n}(\mathbf{x}) \times \mathbf{E}^{0a}(\mathbf{p}) \exp(i\mathbf{k}_p^{0a} \cdot \mathbf{r}_x) \\ & = \sum_{a=\pm} \int \frac{d^2\mathbf{p}}{(2\pi)^2} \mathbf{n}(\mathbf{x}) \times \mathbf{E}^{1a}(\mathbf{p}) \exp(i\mathbf{k}_p^{1a} \cdot \mathbf{r}_x), \end{aligned} \quad (20)$$

$$\begin{aligned} & \frac{\epsilon_0}{\epsilon_1} \sum_{a=\pm} \int \frac{d^2\mathbf{p}}{(2\pi)^2} \mathbf{n}(\mathbf{x}) \cdot \mathbf{E}^{0a}(\mathbf{p}) \exp(i\mathbf{k}_p^{0a} \cdot \mathbf{r}_x) \\ & = \sum_{a=\pm} \int \frac{d^2\mathbf{p}}{(2\pi)^2} \mathbf{n}(\mathbf{x}) \cdot \mathbf{E}^{1a}(\mathbf{p}) \exp(i\mathbf{k}_p^{1a} \cdot \mathbf{r}_x), \end{aligned} \quad (21)$$

$$\begin{aligned} & \sum_{a=\pm} \int \frac{d^2\mathbf{p}}{(2\pi)^2} \mathbf{n}(\mathbf{x}) \times [\mathbf{k}_p^{0a} \times \mathbf{E}^{0a}(\mathbf{p})] \exp(i\mathbf{k}_p^{0a} \cdot \mathbf{r}_x) \\ & = \sum_{a=\pm} \int \frac{d^2\mathbf{p}}{(2\pi)^2} \mathbf{n}(\mathbf{x}) \times [\mathbf{k}_p^{1a} \times \mathbf{E}^{1a}(\mathbf{p})] \exp(i\mathbf{k}_p^{1a} \cdot \mathbf{r}_x), \end{aligned} \quad (22)$$

$$\mathbf{r}_x = \mathbf{x} + h(\mathbf{x}) \hat{\mathbf{e}}_z, \quad \mathbf{k}_p^{0a} \equiv \mathbf{p} + a \alpha_0(\mathbf{p}) \hat{\mathbf{e}}_z,$$

$$\mathbf{k}_p^{1a} \equiv \mathbf{p} + a \alpha_1(\mathbf{p}) \hat{\mathbf{e}}_z, \quad (23)$$

where the summation includes the two possible signs  $a = \pm$ , linked to the propagation directions. We will also use the condition  $\nabla \cdot \mathbf{E}^0(\mathbf{x}, z) = \nabla \cdot \mathbf{E}^1(\mathbf{x}, z)$ , which gives the relation

$$\begin{aligned} & \sum_{a=\pm} \int \frac{d^2\mathbf{p}}{(2\pi)^2} \mathbf{k}_p^{0a} \cdot \mathbf{E}^{0a}(\mathbf{p}) \exp(i\mathbf{k}_p^{0a} \cdot \mathbf{r}_x) \\ & = \sum_{a=\pm} \int \frac{d^2\mathbf{p}}{(2\pi)^2} \mathbf{k}_p^{1a} \cdot \mathbf{E}^{1a}(\mathbf{p}) \exp(i\mathbf{k}_p^{1a} \cdot \mathbf{r}_x). \end{aligned} \quad (24)$$

## B. Field elimination

Equations (20)–(22) and (24) are all linear in the fields  $\mathbf{E}^{0-}$ ,  $\mathbf{E}^{0+}$ ,  $\mathbf{E}^{1-}$ , and  $\mathbf{E}^{1+}$ . In order to eliminate  $\mathbf{E}^{1-}$  or  $\mathbf{E}^{1+}$  in Eqs. (20)–(22) and (24), we will take the following linear combination of their left and right sides:

$$\begin{aligned} & \int d^2\mathbf{x} \{ \mathbf{k}_u^{1b} \times [\text{Eq. (20)}] + [\text{Eq. (22)}] - \mathbf{k}_u^{1b} [\text{Eq. (21)}] \\ & - \mathbf{n}(\mathbf{x}) [\text{Eq. (24)}] \} \exp(-i\mathbf{k}_u^{1b} \cdot \mathbf{r}_x), \end{aligned} \quad (25)$$

with  $\mathbf{k}_u^{1b} \equiv \mathbf{u} + b \alpha_1(\mathbf{u}) \hat{\mathbf{e}}_z$ , and where  $b = \pm$ , has to be fixed according to the choice of the field we want to eliminate. With the vectorial identity  $\mathbf{a} \times (\mathbf{b} \times \mathbf{c}) = \mathbf{b}(\mathbf{a} \cdot \mathbf{c}) - \mathbf{c}(\mathbf{a} \cdot \mathbf{b})$ , the right side of Eq. (25) can be written

$$\begin{aligned} \sum_{a=\pm} \int \int d^2\mathbf{x} \frac{d^2\mathbf{p}}{(2\pi)^2} & [-(\mathbf{k}_u^{1b} + \mathbf{k}_p^{1a}) \cdot \mathbf{n}(\mathbf{x}) \mathbf{E}^{1a}(\mathbf{p}) \\ & + (\mathbf{k}_u^{1b} - \mathbf{k}_p^{1a}) \cdot \mathbf{E}^{1a}(\mathbf{p}) \mathbf{n}(\mathbf{x}) - \mathbf{n}(\mathbf{x}) \cdot \mathbf{E}^{1a}(\mathbf{p}) \\ & \times (\mathbf{k}_u^{1b} - \mathbf{k}_p^{1a})] \exp[-i(\mathbf{k}_u^{1b} - \mathbf{k}_p^{1a}) \cdot \mathbf{r}_x]. \end{aligned} \quad (26)$$

We now have to discuss the different cases depending on the relative sign between  $a$  and  $b$ .

(1) If  $a = -b$ , we can use an integration by parts (see Appendix A) to evaluate  $\mathbf{n}(\mathbf{x}) \equiv \hat{\mathbf{e}}_z - \nabla h(\mathbf{x})$ . Then we can make the replacement

$$\mathbf{n}(\mathbf{x}) = \hat{\mathbf{e}}_z - \nabla h(\mathbf{x}) \leftrightarrow \mathbf{n}(\mathbf{x}) = \hat{\mathbf{e}}_z + \frac{(\mathbf{u} - \mathbf{p})}{[b\alpha_1(\mathbf{u}) - a\alpha_1(\mathbf{p})]}. \quad (27)$$

It has to be noted that the denominator  $[b\alpha_1(\mathbf{u}) - a\alpha_1(\mathbf{p})]$  does not present any singularity because  $a = -b$ . For the first term in integral (26), we obtain

$$\begin{aligned} & -(\mathbf{k}_u^{1b} + \mathbf{k}_p^{1a}) \cdot \mathbf{n}(\mathbf{x}) \mathbf{E}^{1a}(\mathbf{p}) \\ & = \frac{-b\mathbf{E}^{1a}(\mathbf{p})}{[\alpha_1(\mathbf{u}) + \alpha_1(\mathbf{p})]} [\mathbf{u}^2 - \mathbf{p}^2 + \alpha_1(\mathbf{u})^2 - \alpha_1(\mathbf{p})^2], \\ & = 0. \end{aligned} \quad (28)$$

The last equality can be easily checked using Eq. (8). For the sum of the second and third terms of Eq. (26), we also have

$$(\mathbf{k}_u^{1b} - \mathbf{k}_p^{1a}) \cdot \mathbf{E}^{1a}(\mathbf{p}) \mathbf{n}(\mathbf{x}) - \mathbf{n}(\mathbf{x}) \cdot \mathbf{E}^{1a}(\mathbf{p}) (\mathbf{k}_u^{1b} - \mathbf{k}_p^{1a}) = 0, \quad (29)$$

due to the fact that

$$\mathbf{n}(\mathbf{x}) = \frac{\mathbf{k}_u^{1b} - \mathbf{k}_p^{1a}}{b\alpha_1(\mathbf{u}) - a\alpha_1(\mathbf{p})}. \quad (30)$$

(2) If  $a = b$ , we can use again the integration by parts only if  $\alpha_1(\mathbf{u}) \neq \alpha_1(\mathbf{p})$ . Then we have to consider three cases: (a)  $\mathbf{u} \neq \mathbf{p}$  and  $\mathbf{u} \neq -\mathbf{p}$ , as in the previous case by using an integration by parts we show that Eq. (26) is zero. (b)  $\mathbf{u} = \mathbf{p}$ ; then  $\mathbf{k}_u^{1b} = \mathbf{k}_p^{1a}$ ,

$$\begin{aligned} & - \int d^2\mathbf{x} (\mathbf{k}_u^{1b} + \mathbf{k}_p^{1a}) \cdot \mathbf{n}(\mathbf{x}) \mathbf{E}^{1a}(\mathbf{p}) \exp[-i(\mathbf{k}_u^{1b} - \mathbf{k}_p^{1a}) \cdot \mathbf{r}_x] \\ & = - \int d^2\mathbf{x} 2\mathbf{k}_u^{1b} \cdot \mathbf{n}(\mathbf{x}) \mathbf{E}^{1a}(\mathbf{p}) \\ & = -2b\alpha_1(\mathbf{u}) \mathbf{E}^{1a}(\mathbf{p}) \int d\mathbf{x} = -2b\alpha_1(\mathbf{u}) L^2 \mathbf{E}^{1a}(\mathbf{p}), \end{aligned} \quad (31)$$

because  $\int d^2\mathbf{x} \nabla h(\mathbf{x}) = 0$ , and

$$(\mathbf{k}_u^{1b} - \mathbf{k}_p^{1a}) \cdot \mathbf{E}^{1a}(\mathbf{p}) \mathbf{n}(\mathbf{x}) - \mathbf{n}(\mathbf{x}) \cdot \mathbf{E}^{1a}(\mathbf{p}) (\mathbf{k}_u^{1b} - \mathbf{k}_p^{1a}) = 0. \quad (32)$$

(c)  $\mathbf{u} = -\mathbf{p} \neq 0$ ; then  $\mathbf{k}_u^{1b} - \mathbf{k}_p^{1a} = 2\mathbf{u}$ ,

and if we denote  $\delta_{\mathbf{u},-\mathbf{p}}$  the kronecker symbol

$$\begin{aligned} & \delta_{\mathbf{u},-\mathbf{p}} \int d^2\mathbf{x} \mathbf{n}(\mathbf{x}) \exp[-i(\mathbf{k}_u^{1b} - \mathbf{k}_p^{1a}) \cdot \mathbf{r}_x] \\ & = \delta_{\mathbf{u},-\mathbf{p}} \int d^2\mathbf{x} [\hat{\mathbf{e}}_z - \nabla h(\mathbf{x})] \exp(-2i\mathbf{u} \cdot \mathbf{x}) \\ & = \delta_{\mathbf{u},-\mathbf{p}} \left\{ \hat{\mathbf{e}}_z \int d^2\mathbf{x} \exp(-2i\mathbf{u} \cdot \mathbf{x}) - \hat{\mathbf{e}}_x \right. \\ & \quad \times \int dy [\exp(-2i\mathbf{u} \cdot \mathbf{x}) h(x,y)]_{x=-L/2}^{x=L/2} - \hat{\mathbf{e}}_y \\ & \quad \times \int dx [\exp(-2i\mathbf{u} \cdot \mathbf{x}) h(x,y)]_{y=-L/2}^{y=L/2} \\ & \quad \left. - 2i\mathbf{u} \int d^2\mathbf{x} h(\mathbf{k}) e^{-2i\mathbf{u} \cdot \mathbf{x}} \right\} \\ & = \delta_{\mathbf{u},-\mathbf{p}} \left[ \hat{\mathbf{e}}_z \frac{\sin u_x L}{u_x} \frac{\sin u_y L}{u_y} - 2i\mathbf{u} h(-2\mathbf{u}) \right] \end{aligned} \quad (33)$$

since  $\mathbf{u} \neq 0$ , the first term of the previous expression is at most of order  $L$  and as

$$\int \frac{d^2\mathbf{p}}{(2\pi)^2} \leftrightarrow \frac{1}{L^2} \sum_{\mathbf{p}},$$

this result implies that expression (26) is also zero when  $L \rightarrow \infty$ .

We can summarize all the above results in the form

$$\begin{aligned} & - \int d^2\mathbf{x} (\mathbf{k}_u^{1b} + \mathbf{k}_p^{1a}) \cdot \mathbf{n}(\mathbf{x}) \mathbf{E}^{1a}(\mathbf{p}) \exp[-i(\mathbf{k}_u^{1b} - \mathbf{k}_p^{1a}) \cdot \mathbf{r}_x] \\ & = -2b\alpha_1(\mathbf{u}) \delta_{a,b} \delta_{\mathbf{u},\mathbf{p}} L^2 \mathbf{E}^{1a}(\mathbf{p}) \\ & = -2b\alpha_1(\mathbf{u}) \delta_{a,b} (2\pi)^2 \delta(\mathbf{u} - \mathbf{p}) \mathbf{E}^{1b}(\mathbf{u}) \end{aligned} \quad (34)$$

when  $L \rightarrow +\infty$ ,

where  $\delta(\mathbf{u} - \mathbf{p}) = L^2 / (2\pi)^2 \delta_{\mathbf{u},\mathbf{p}}$  the Dirac function.

After an integration on  $\mathbf{p}$  and a summation on  $a$ , for expression (26) we obtain

$$-2b\alpha_1(\mathbf{u}) \mathbf{E}^{1b}(\mathbf{u}). \quad (35)$$

We see that we can eliminate the field  $\mathbf{E}^{1-}(\mathbf{u})$  or  $\mathbf{E}^{1+}(\mathbf{u})$  depending on the choice made for  $b = \pm$ .

Now, if we consider the *left side* of Eq. (25), we have

$$\begin{aligned} & \sum_{a=\pm} \int \int d^2\mathbf{x} \frac{d^2\mathbf{p}}{(2\pi)^2} \left[ -(\mathbf{k}_u^{1b} + \mathbf{k}_p^{0a}) \cdot \mathbf{n}(\mathbf{x}) \mathbf{E}^{0a}(\mathbf{p}) \right. \\ & \quad + (\mathbf{k}_u^{1b} - \mathbf{k}_p^{0a}) \cdot \mathbf{E}^{0a}(\mathbf{p}) \mathbf{n}(\mathbf{x}) - \mathbf{n}(\mathbf{x}) \cdot \mathbf{E}^{0a}(\mathbf{p}) \\ & \quad \left. \times \left( \frac{\epsilon_0}{\epsilon_1} \mathbf{k}_u^{1b} - \mathbf{k}_p^{0a} \right) \right] \exp[-i(\mathbf{k}_u^{1b} - \mathbf{k}_p^{0a}) \cdot \mathbf{r}_x]. \end{aligned} \quad (36)$$

Using an integration by parts, we replace  $\mathbf{n}(\mathbf{x})$  by Eq. (27):

$$\mathbf{n}(\mathbf{x}) \leftrightarrow \hat{\mathbf{e}}_z + \frac{(\mathbf{u} - \mathbf{p})}{[b\alpha_1(\mathbf{u}) - a\alpha_0(\mathbf{p})]} = \frac{\mathbf{k}_u^{1b} - \mathbf{k}_p^{0a}}{[b\alpha_1(\mathbf{u}) - a\alpha_0(\mathbf{p})]}. \quad (37)$$

In this case there is no need to discuss the relative sign between  $a$  and  $b$  because  $b\alpha_1(\mathbf{u}) - a\alpha_0(\mathbf{p}) \neq 0$ , due to the fact that  $\epsilon_0 \neq \epsilon_1$ . We then obtain

$$\begin{aligned} & -(\mathbf{k}_u^{1b} + \mathbf{k}_p^{1a}) \cdot \mathbf{n}(\mathbf{x}) \mathbf{E}^{0a}(\mathbf{p}) \\ &= -\frac{\mathbf{u}^2 - \mathbf{p}^2 + \alpha_1(\mathbf{u})^2 - \alpha_0(\mathbf{p})^2}{b\alpha_1(\mathbf{u}) - a\alpha_0(\mathbf{p})} \mathbf{E}^{0a}(\mathbf{p}), \\ &= -\frac{(\epsilon_1 - \epsilon_0)K_0^2}{b\alpha_1(\mathbf{u}) - a\alpha_0(\mathbf{p})} \mathbf{E}^{0a}(\mathbf{p}), \end{aligned} \quad (38)$$

where we have used definitions (4) and (8). The remaining terms of Eq. (36) give

$$\begin{aligned} & (\mathbf{k}_u^{1b} - \mathbf{k}_p^{0a}) \cdot \mathbf{E}^{0a}(\mathbf{p}) \mathbf{n}(\mathbf{x}) - \mathbf{n}(\mathbf{x}) \cdot \mathbf{E}^{0a}(\mathbf{p}) \left( \frac{\epsilon_0}{\epsilon_1} \mathbf{k}_u^{1b} - \mathbf{k}_p^{0a} \right) \\ &= (\mathbf{k}_u^{1b} - \mathbf{k}_p^{0a}) \cdot \mathbf{E}^{0a}(\mathbf{p}) \mathbf{n}(\mathbf{x}) - \mathbf{n}(\mathbf{x}) \cdot \mathbf{E}^{0a}(\mathbf{p}) (\mathbf{k}_u^{1b} - \mathbf{k}_p^{0a}) \\ &+ \mathbf{n}(\mathbf{x}) \cdot \mathbf{E}^{0a}(\mathbf{p}) \left( \mathbf{k}_u^{1b} - \frac{\epsilon_0}{\epsilon_1} \mathbf{k}_u^{1b} \right) \\ &= \frac{\mathbf{k}_u^{1b} - \mathbf{k}_p^{0a}}{b\alpha_1(\mathbf{u}) - a\alpha_0(\mathbf{p})} \cdot \mathbf{E}^{0a}(\mathbf{p}) \frac{(\epsilon_1 - \epsilon_0)}{\epsilon_1} \mathbf{k}_u^{1b}. \end{aligned} \quad (39)$$

Introducing the notation

$$I[\alpha|\mathbf{p}] \equiv \int d^2\mathbf{x} \exp[-i\mathbf{p} \cdot \mathbf{x} - i\alpha h(\mathbf{x})], \quad (40)$$

and taking into account expressions (35), (38), and (39), we express the resulting linear combination [Eq. (25)] in the form

$$\begin{aligned} & \sum_{a=\pm} \int \frac{d^2\mathbf{p}}{(2\pi)^2} \frac{I[b\alpha_1(\mathbf{u}) - a\alpha_0(\mathbf{p})|\mathbf{u} - \mathbf{p}]}{b\alpha_1(\mathbf{u}) - a\alpha_0(\mathbf{p})} \\ & \times \left[ K_0^2 \mathbf{E}^{0a}(\mathbf{p}) - \frac{\mathbf{k}_u^{1b}}{\epsilon_1} (\mathbf{k}_u^{1b} - \mathbf{k}_p^{0a}) \cdot \mathbf{E}^{0a}(\mathbf{p}) \right] \\ &= \frac{2b\alpha_1(\mathbf{u})}{(\epsilon_1 - \epsilon_0)} \mathbf{E}^{1b}(\mathbf{u}), \end{aligned} \quad (41)$$

this expression represents a set of two equations, depending on the choice for  $b = \pm$ . The last step is to project Eq. (41) on the natural basis of  $\mathbf{E}^{1b}(\mathbf{u})$ , namely,  $[\mathbf{u}]^{1b} \equiv [\hat{\mathbf{e}}_V^{1b}(\mathbf{u}), \hat{\mathbf{e}}_H(\mathbf{u})]$ , which has the property to be orthogonal to  $\mathbf{k}_u^{1b}$ , so it eliminates the second term of Eq. (41), left hand side. Let us note that in order to decompose  $\mathbf{E}^{0a}(\mathbf{p})$  on  $[\mathbf{p}]^{0a}$ , one has to define a matrix  $\bar{\mathbf{M}}^{1b,0a}(\mathbf{u}|\mathbf{p})$  transforming a vector expressed on the basis  $[\mathbf{p}]^{0a}$  into a vector on the basis  $[\mathbf{u}]^{1b}$ , multiplied by a numerical factor  $(\epsilon_0\epsilon_1)^{1/2}K_0^2$  introduced for a matter of convenience:

$$\bar{\mathbf{M}}^{1b,0a}(\mathbf{u}|\mathbf{p}) \equiv (\epsilon_0\epsilon_1)^{1/2}K_0^2 \begin{pmatrix} \hat{\mathbf{e}}_V^{1b}(\mathbf{u}) \cdot \hat{\mathbf{e}}_V^{0a}(\mathbf{p}) & \hat{\mathbf{e}}_V^{1b}(\mathbf{u}) \cdot \hat{\mathbf{e}}_H(\mathbf{p}) \\ \hat{\mathbf{e}}_H(\mathbf{u}) \cdot \hat{\mathbf{e}}_V^{0a}(\mathbf{p}) & \hat{\mathbf{e}}_H(\mathbf{u}) \cdot \hat{\mathbf{e}}_H(\mathbf{p}) \end{pmatrix} \quad (42)$$

### C. Reduced Rayleigh equations

With definitions (11)–(14) the matrix  $\bar{\mathbf{M}}$  takes the form

$$\bar{\mathbf{M}}^{1b,0a}(\mathbf{u}|\mathbf{p}) = \begin{pmatrix} \|\mathbf{u}\|\|\mathbf{p}\| + ab\alpha_1(\mathbf{u})\alpha_0(\mathbf{p})\hat{\mathbf{u}} \cdot \hat{\mathbf{p}} & -b\epsilon_0^{1/2}K_0\alpha_1(\mathbf{u})(\hat{\mathbf{u}} \times \hat{\mathbf{p}})_z \\ a\epsilon_1^{1/2}K_0\alpha_0(\mathbf{p})(\hat{\mathbf{u}} \times \hat{\mathbf{p}})_z & (\epsilon_0\epsilon_1)^{1/2}K_0^2\hat{\mathbf{u}} \cdot \hat{\mathbf{p}} \end{pmatrix}, \quad (43)$$

and the two reduced Raleigh equations resulting from Eq. (41) read

$$\sum_{a=\pm} \int \frac{d^2\mathbf{p}}{(2\pi)^2} \frac{I[b\alpha_1(\mathbf{u}) - a\alpha_0(\mathbf{p})|\mathbf{u} - \mathbf{p}]}{b\alpha_1(\mathbf{u}) - a\alpha_0(\mathbf{p})} \bar{\mathbf{M}}^{1b,0a}(\mathbf{u}|\mathbf{p}) \mathbf{E}^{0a}(\mathbf{p}) = \frac{2b(\epsilon_0\epsilon_1)^{1/2}\alpha_1(\mathbf{u})}{(\epsilon_1 - \epsilon_0)} \mathbf{E}^{1b}(\mathbf{u}), \quad (44)$$

where we suppose that  $\mathbf{E}^{0a}(\mathbf{p})$  and  $\mathbf{E}^{1b}(\mathbf{u})$ , respectively, are decomposed on the bases  $[\mathbf{p}]^{0a}$  and  $[\mathbf{u}]^{1b}$ . We can derive a similar equation where  $\mathbf{E}^{0b}$  is now eliminated, by simply exchanging  $\epsilon_0$  and  $\epsilon_1$  in Eqs. (43) and (44). Due to the symmetry of Eqs. (3), (7) and (17)–(19), we obtain

$$\sum_{a=\pm} \int \frac{d^2\mathbf{p}}{(2\pi)^2} \frac{I[b\alpha_0(\mathbf{u}) - a\alpha_1(\mathbf{p})|\mathbf{u} - \mathbf{p}]}{b\alpha_0(\mathbf{u}) - a\alpha_1(\mathbf{p})} \bar{\mathbf{M}}^{0b,1a}(\mathbf{u}|\mathbf{p}) \mathbf{E}^{1a}(\mathbf{p}) = -\frac{2b(\epsilon_0\epsilon_1)^{1/2}\alpha_0(\mathbf{u})}{(\epsilon_1 - \epsilon_0)} \mathbf{E}^{0b}(\mathbf{u}), \quad (45)$$

$$\bar{\mathbf{M}}^{0b,1a}(\mathbf{u}|\mathbf{p}) = \begin{pmatrix} \|\mathbf{u}\|\|\mathbf{p}\| + ab\alpha_0(\mathbf{u})\alpha_1(\mathbf{p})\hat{\mathbf{u}} \cdot \hat{\mathbf{p}} & -b\epsilon_1^{1/2}K_0\alpha_0(\mathbf{u})(\hat{\mathbf{u}} \times \hat{\mathbf{p}})_z \\ a\epsilon_0^{1/2}K_0\alpha_1(\mathbf{p})(\hat{\mathbf{u}} \times \hat{\mathbf{p}})_z & (\epsilon_0\epsilon_1)^{1/2}K_0^2\hat{\mathbf{u}} \cdot \hat{\mathbf{p}} \end{pmatrix}. \quad (46)$$

In Sec. III we will show how these equations greatly simplify the perturbative calculation of plane-wave scattering by a rough surface. In order to keep a compact notation, we introduce matrices  $\bar{\mathbf{M}}_h$  given by

$$\bar{\mathbf{M}}_h^{1b,0a}(\mathbf{u}|\mathbf{p}) \equiv \frac{I[b\alpha_1(\mathbf{u}) - a\alpha_0(\mathbf{p})|\mathbf{u}-\mathbf{p}]}{b\alpha_1(\mathbf{u}) - a\alpha_0(\mathbf{p})} \bar{\mathbf{M}}^{1b,0a}(\mathbf{u}|\mathbf{p}), \quad (47)$$

$$\bar{\mathbf{M}}_h^{0b,1a}(\mathbf{u}|\mathbf{p}) \equiv \frac{I[b\alpha_0(\mathbf{u}) - a\alpha_1(\mathbf{p})|\mathbf{u}-\mathbf{p}]}{b\alpha_0(\mathbf{u}) - a\alpha_1(\mathbf{p})} \bar{\mathbf{M}}^{0b,1a}(\mathbf{u}|\mathbf{p}). \quad (48)$$

### III. DIFFUSION MATRIX

We are interested in the diffusion of an incident plane wave by a rough surface from the previous formalism. We define an incident plane wave of wave vector  $\mathbf{k}_{\mathbf{p}_0}^{0-}$  as

$$\mathbf{E}^{0-}(\mathbf{p}) = (2\pi)^2 \delta(\mathbf{p} - \mathbf{p}_0) \mathbf{E}^i(\mathbf{p}_0). \quad (49)$$

We are naturally led to introduce the diffusion operator  $\bar{\mathbf{R}}$ ,

$$\mathbf{E}^{0+}(\mathbf{p}) \equiv \bar{\mathbf{R}}(\mathbf{p}|\mathbf{p}_0) \cdot \mathbf{E}^i(\mathbf{p}_0), \quad (50)$$

which can be represented in a matrix form, using the vectorial basis described above:

$$\bar{\mathbf{R}}(\mathbf{p}|\mathbf{p}_0) = \begin{pmatrix} R_{VV}(\mathbf{p}|\mathbf{p}_0) & R_{VH}(\mathbf{p}|\mathbf{p}_0) \\ R_{HV}(\mathbf{p}|\mathbf{p}_0) & R_{HH}(\mathbf{p}|\mathbf{p}_0) \end{pmatrix}_{[\mathbf{p}_0^-] \rightarrow [\mathbf{p}^+]}. \quad (51)$$

The field in medium 0 is now written [using decomposition (3)]

$$\mathbf{E}^0(\mathbf{r}) = \mathbf{E}^i(\mathbf{p}_0) \exp(i\mathbf{k}_{\mathbf{p}_0}^{0-} \cdot \mathbf{r}) + \int \frac{d^2\mathbf{p}}{(2\pi)^2} \bar{\mathbf{R}}(\mathbf{p}|\mathbf{p}_0) \cdot \mathbf{E}^i(\mathbf{p}_0) \exp(i\mathbf{k}_{\mathbf{p}}^{0+} \cdot \mathbf{r}). \quad (51)$$

### IV. A PERTURBATIVE DEVELOPMENT

In order to obtain a perturbative development, one has to make a perturbative analysis of the given boundary-problem. A direct approach which uses an exact integral equation called the extended boundary condition (see Refs. 4 and 26) requires tedious calculations. Another issue is to use the Rayleigh hypothesis in the boundary conditions. This is the method generally used to obtain the SPM.<sup>12,13,15</sup> But a great deal of simplification can be achieved if we are only interested in the field outside the slab. It was discovered by Brown *et al.*<sup>16</sup> that an exact integral equation can be obtained (excepted for the Rayleigh hypothesis), which only involves the scattering matrix  $\bar{\mathbf{R}}(\mathbf{p}|\mathbf{p}_0)$ . The proof is based on the extinction theorem, which decouples the fields inside and outside the media. In this section, we will show how to obtain this integral equation from the previous development, including a generalization to the case of bounded random media. We seek for a perturbative development of  $\bar{\mathbf{R}}$  in powers of the height  $h$ :

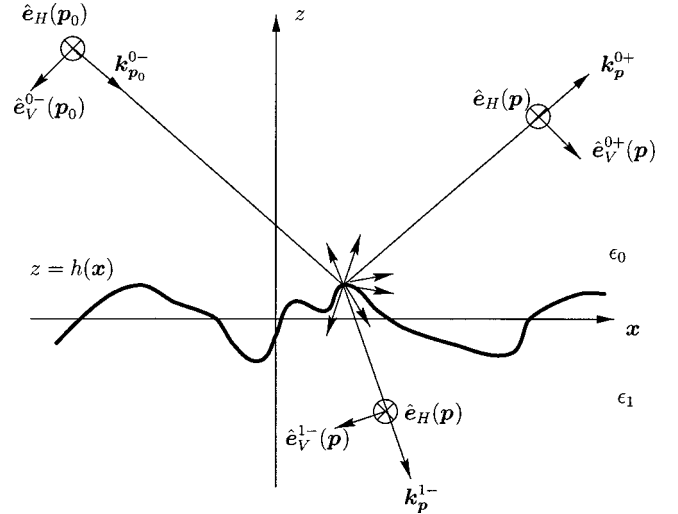


FIG. 3. A two-dimensional rough surface separating two dielectric media 0 and 1.

$$\bar{\mathbf{R}}(\mathbf{p}|\mathbf{p}_0) = \bar{\mathbf{R}}^{(0)}(\mathbf{p}|\mathbf{p}_0) + \bar{\mathbf{R}}^{(1)}(\mathbf{p}|\mathbf{p}_0) + \bar{\mathbf{R}}^{(2)}(\mathbf{p}|\mathbf{p}_0) + \bar{\mathbf{R}}^{(3)}(\mathbf{p}|\mathbf{p}_0) + \dots \quad (52)$$

One can easily prove that this development takes the form (see Appendix B).

$$\begin{aligned} \bar{\mathbf{R}}(\mathbf{p}|\mathbf{p}_0) &= (2\pi)^2 \delta(\mathbf{p} - \mathbf{p}_0) \bar{\mathbf{X}}^{(0)}(\mathbf{p}_0) \\ &+ \alpha_0(\mathbf{p}_0) \bar{\mathbf{X}}^{(1)}(\mathbf{p}|\mathbf{p}_0) h(\mathbf{p} - \mathbf{p}_0) \\ &+ \alpha_0(\mathbf{p}_0) \int \frac{d^2\mathbf{p}_1}{(2\pi)^2} \bar{\mathbf{X}}^{(2)}(\mathbf{p}|\mathbf{p}_1|\mathbf{p}_0) h(\mathbf{p} - \mathbf{p}_1) \\ &h(\mathbf{p}_1 - \mathbf{p}_0) + \alpha_0(\mathbf{p}_0) \int \int \frac{d^2\mathbf{p}_1}{(2\pi)^2} \frac{d^2\mathbf{p}_2}{(2\pi)^2} \\ &\bar{\mathbf{X}}^{(3)}(\mathbf{p}|\mathbf{p}_1|\mathbf{p}_2|\mathbf{p}_0) h(\mathbf{p} - \mathbf{p}_1) h(\mathbf{p}_1 - \mathbf{p}_2) \\ &h(\mathbf{p}_2 - \mathbf{p}_0), \end{aligned} \quad (53)$$

where  $h(\mathbf{p})$  is the Fourier transform<sup>28</sup> of  $h(\mathbf{x})$ :

$$h(\mathbf{p}) \equiv \int d^2\mathbf{x} \exp(-i\mathbf{p} \cdot \mathbf{x}) h(\mathbf{x}). \quad (54)$$

We will now show the power of the reduced Rayleigh equation for the three configurations mentioned in the Introduction.

#### A. A rough surface separating two different media

We consider a rough surface delimiting two media which are semi-infinite; see Fig. 3. We suppose that there is no upward field propagating in the medium 1, so  $\mathbf{E}^{1+} = 0$ . With the choice  $b = +$  in Eq. (44), we obtain the following integral equation for the scattering matrix  $\bar{\mathbf{R}}_{s\epsilon_0, \epsilon_1}(\mathbf{p}|\mathbf{p}_0)$  for a single surface<sup>29</sup> (the subscript  $s$  means a single surface located at  $z=0$ ):

$$\int \frac{d^2\mathbf{p}}{(2\pi)^2} \bar{\mathbf{M}}_h^{1+,0+}(\mathbf{u}|\mathbf{p}) \cdot \bar{\mathbf{R}}_{s\epsilon_0,\epsilon_1}(\mathbf{p}|\mathbf{p}_0) + \bar{\mathbf{M}}_h^{1+,0-}(\mathbf{u}|\mathbf{p}) = 0. \quad (55)$$

[This equation was already obtained by making use of the extinction theorem.<sup>16</sup> It should be noted that since the right-hand side of Eq. (55) is null, one can simplify the second line of the matrices,  $\bar{\mathbf{M}}^{1+,0+}$  and  $\bar{\mathbf{M}}^{1+,0-}$ , by a factor  $(\epsilon_1)^{1/2}$ , then they coincide with the  $\bar{\mathbf{M}}$  and  $\bar{\mathbf{N}}$  matrices derived by Brown *et al.*<sup>16</sup>]

In order to construct a perturbative development, the method is simply to expand in Taylor series the term  $\exp[i\alpha h(\mathbf{x})]$  inside  $I[\alpha|\mathbf{p}]$  [Eq. (40)],

$$I[\alpha|\mathbf{p}] = (2\pi)^2 \delta(\mathbf{p}) - i\alpha h^{(1)}(\mathbf{p}) - \frac{\alpha^2}{2} h^{(2)}(\mathbf{p}) - \frac{i\alpha^3}{3!} h^{(3)}(\mathbf{p}) + \dots, \quad (56)$$

$$h^{(n)}(\mathbf{p}) \equiv \int d^2\mathbf{x} \exp(-i\mathbf{p}\cdot\mathbf{x}) h^n(\mathbf{x}), \quad (57)$$

and to collect the terms of the same order in  $h(\mathbf{x})$ . Let us define the matrix

$$\bar{\mathbf{D}}_{10}^{\pm}(\mathbf{p}_0) \equiv \begin{pmatrix} \epsilon_1 \alpha_0(\mathbf{p}_0) \pm \epsilon_0 \alpha_1(\mathbf{p}_0) & 0 \\ 0 & \alpha_0(\mathbf{p}_0) \pm \alpha_1(\mathbf{p}_0) \end{pmatrix}, \quad (58)$$

the classical specular reflection coefficients for TM and TE waves are given by the diagonal elements of the matrix:

$$\bar{\mathbf{V}}^{10}(\mathbf{p}_0) \equiv \bar{\mathbf{D}}_{10}^{-}(\mathbf{p}_0) \cdot [\bar{\mathbf{D}}_{10}^{+}(\mathbf{p}_0)]^{-1}. \quad (59)$$

Introducing Eq. (56) into Eq. (55), for  $\bar{\mathbf{R}}_{s\epsilon_0,\epsilon_1}$  we obtain a perturbative development of the form of Eq. (53), where the coefficients are given by

$$\begin{aligned} \bar{\mathbf{X}}_{s\epsilon_0,\epsilon_1}^{(0)}(\mathbf{p}_0) &= -\frac{\alpha_1(\mathbf{p}_0) - \alpha_0(\mathbf{p}_0)}{\alpha_1(\mathbf{p}_0) + \alpha_0(\mathbf{p}_0)} \\ &\times [\bar{\mathbf{M}}^{1+,0+}(\mathbf{p}_0|\mathbf{p}_0)]^{-1} \cdot \bar{\mathbf{M}}^{1+,0-}(\mathbf{p}_0|\mathbf{p}_0) \\ &= \bar{\mathbf{V}}^{10}(\mathbf{p}_0) \end{aligned} \quad (60)$$

and

$$\bar{\mathbf{X}}_{s\epsilon_0,\epsilon_1}^{(1)}(\mathbf{u}|\mathbf{p}_0) = 2i\bar{\mathbf{Q}}^+(\mathbf{u}|\mathbf{p}_0), \quad (61)$$

$$\begin{aligned} \bar{\mathbf{X}}_{s\epsilon_0,\epsilon_1}^{(2)}(\mathbf{u}|\mathbf{p}_1|\mathbf{p}_0) &= \alpha_1(\mathbf{u})\bar{\mathbf{Q}}^+(\mathbf{u}|\mathbf{p}_0) + \alpha_0(\mathbf{p}_0)\bar{\mathbf{Q}}^-(\mathbf{u}|\mathbf{p}_0) \\ &\quad - 2\bar{\mathbf{P}}(\mathbf{u}|\mathbf{p}_1) \cdot \bar{\mathbf{Q}}^+(\mathbf{p}_1|\mathbf{p}_0), \end{aligned} \quad (62)$$

$$\begin{aligned} \bar{\mathbf{X}}_{s\epsilon_0,\epsilon_1}^{(3)}(\mathbf{u}|\mathbf{p}_1|\mathbf{p}_2|\mathbf{p}_0) &= -\frac{i}{3} [[\alpha_1^2(\mathbf{u}) + \alpha_0^2(\mathbf{p}_0)]\bar{\mathbf{Q}}^+(\mathbf{u}|\mathbf{p}_0) \\ &\quad + 2\alpha_1(\mathbf{u})\alpha_0(\mathbf{p}_0)\bar{\mathbf{Q}}^-(\mathbf{u}|\mathbf{p}_0)] \\ &\quad + i\bar{\mathbf{P}}(\mathbf{u}|\mathbf{p}_1) \cdot \bar{\mathbf{X}}_{s\epsilon_0,\epsilon_1}^{(2)}(\mathbf{p}_1|\mathbf{p}_2|\mathbf{p}_0) \\ &\quad + i[\alpha_1(\mathbf{u}) \\ &\quad - \alpha_0(\mathbf{p}_2)] \cdot \bar{\mathbf{P}}(\mathbf{u}|\mathbf{p}_2) \cdot \bar{\mathbf{Q}}^+(\mathbf{p}_2|\mathbf{p}_0), \end{aligned} \quad (63)$$

with

$$\begin{aligned} \bar{\mathbf{Q}}^{\pm}(\mathbf{u}|\mathbf{p}_0) &\equiv \frac{\alpha_1(\mathbf{u}) - \alpha_0(\mathbf{p}_0)}{2\alpha_0(\mathbf{p}_0)} [\bar{\mathbf{M}}^{1+,0+}(\mathbf{u}|\mathbf{u})]^{-1} \cdot [\bar{\mathbf{M}}^{1+,0-}(\mathbf{u}|\mathbf{p}_0) \\ &\quad \pm \bar{\mathbf{M}}^{1+,0+}(\mathbf{u}|\mathbf{p}_0) \cdot \bar{\mathbf{X}}^{(0)}(\mathbf{p}_0)], \end{aligned} \quad (64)$$

$$\begin{aligned} \bar{\mathbf{P}}(\mathbf{u}|\mathbf{p}_1) &\equiv [\alpha_1(\mathbf{u}) - \alpha_0(\mathbf{u})] \\ &\quad \times [\bar{\mathbf{M}}^{1+,0+}(\mathbf{u}|\mathbf{u})]^{-1} \cdot [\bar{\mathbf{M}}^{1+,0+}(\mathbf{u}|\mathbf{p}_1)]. \end{aligned} \quad (65)$$

After some simple algebra, we obtain

$$\bar{\mathbf{Q}}^+(\mathbf{u}|\mathbf{p}_0) = (\epsilon_1 - \epsilon_0) [\bar{\mathbf{D}}_{10}^+(\mathbf{u})]^{-1} \cdot \begin{pmatrix} \epsilon_1 \|\mathbf{u}\| \|\mathbf{p}_0\| - \epsilon_0 \alpha_1(\mathbf{u}) \alpha_1(\mathbf{p}_0) \hat{\mathbf{u}} \cdot \hat{\mathbf{p}}_0 & -\epsilon_1^{1/2} K_0 \alpha_1(\mathbf{u}) (\hat{\mathbf{u}} \times \hat{\mathbf{p}}_0)_z \\ -\epsilon_0^{1/2} K_0 \alpha_1(\mathbf{p}_0) (\hat{\mathbf{u}} \times \hat{\mathbf{p}}_0)_z & K_0^2 \hat{\mathbf{u}} \cdot \hat{\mathbf{p}}_0 \end{pmatrix} \cdot [\bar{\mathbf{D}}_{10}^+(\mathbf{p}_0)]^{-1}, \quad (66)$$

$$\bar{\mathbf{Q}}^-(\mathbf{u}|\mathbf{p}_0) = \frac{(\epsilon_1 - \epsilon_0)}{\alpha_0(\mathbf{p}_0)} [\bar{\mathbf{D}}_{10}^+(\mathbf{u})]^{-1} \cdot \begin{pmatrix} \epsilon_0 \alpha_1(\mathbf{p}_0) \|\mathbf{u}\| \|\mathbf{p}_0\| - \epsilon_1 \alpha_1(\mathbf{u}) \alpha_0^2(\mathbf{p}_0) \hat{\mathbf{u}} \cdot \hat{\mathbf{p}}_0 & -\epsilon_0^{1/2} K_0 \alpha_1(\mathbf{u}) \alpha_1(\mathbf{p}_0) (\hat{\mathbf{u}} \times \hat{\mathbf{p}}_0)_z \\ -\epsilon_0^{-1/2} \epsilon_1 K_0 \alpha_0^2(\mathbf{p}_0) (\hat{\mathbf{u}} \times \hat{\mathbf{p}}_0)_z & K_0^2 \alpha_1(\mathbf{p}_0) \hat{\mathbf{u}} \cdot \hat{\mathbf{p}}_0 \end{pmatrix} \cdot [\bar{\mathbf{D}}_{10}^+(\mathbf{p}_0)]^{-1}, \quad (67)$$

$$\bar{\mathbf{P}}(\mathbf{u}|\mathbf{p}_1) = (\epsilon_1 - \epsilon_0) [\bar{\mathbf{D}}_{10}^+(\mathbf{u})]^{-1} \cdot \begin{pmatrix} \|\mathbf{u}\| \|\mathbf{p}_1\| + \alpha_1(\mathbf{u}) \alpha_0(\mathbf{p}_1) \hat{\mathbf{u}} \cdot \hat{\mathbf{p}}_1 & -\epsilon_0^{1/2} K_0 \alpha_1(\mathbf{u}) (\hat{\mathbf{u}} \times \hat{\mathbf{p}}_1)_z \\ \epsilon_0^{-1/2} K_0 \alpha_0(\mathbf{p}_1) (\hat{\mathbf{u}} \times \hat{\mathbf{p}}_1)_z & K_0^2 \hat{\mathbf{u}} \cdot \hat{\mathbf{p}}_1 \end{pmatrix}. \quad (68)$$

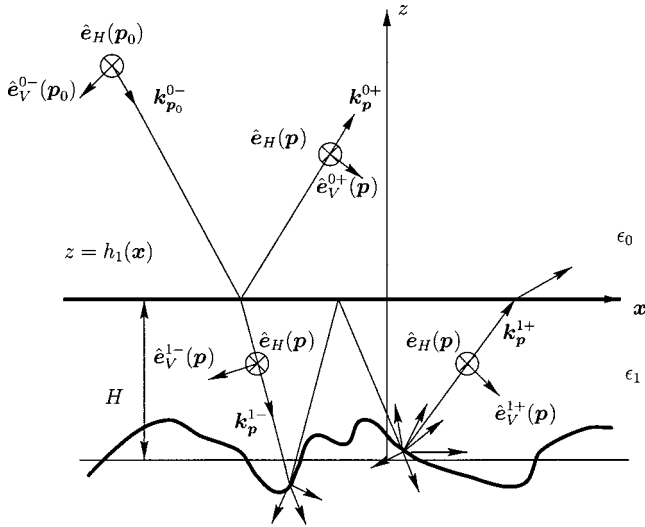


FIG. 4. A slab formed with a bottom two-dimensional rough surface and an upper planar surface.

It can be easily checked that  $\bar{\mathbf{X}}^{(1)}$  is the well-known first-order term in perturbation theory which was obtained by Rice.<sup>12</sup> After some lengthy calculations, we have proven that Eqs. (62) and (63), are identical to those found by Johnson.<sup>13</sup> Thus our expressions (62) and (63), are a compact manner in which to write the second and third-order terms of the perturbative expansion; moreover, they are well adapted for numerical computations. However, it has to be noted that only the first term  $\bar{\mathbf{X}}^{(1)}$  is reciprocal. Since the second- and third-order perturbative terms are included in the integral, the coefficient  $\bar{\mathbf{X}}^{(2)}$  and  $\bar{\mathbf{X}}^{(3)}$ , are not unique; however, they can be put into a reciprocal form (see Appendix B).

It is worth noticing that we can follow an analogous procedure to calculate the transmitted field. By taking  $b = -$  in Eq. (45), we obtain

$$\int \frac{d^2 \mathbf{p}}{(2\pi)^2} \bar{\mathbf{M}}_h^{0^-, 1^-}(\mathbf{u}|\mathbf{p}) \cdot \mathbf{E}^{1^-}(\mathbf{p}) = \frac{2(\epsilon_0 \epsilon_1)^{1/2} \alpha_0(\mathbf{u})}{(\epsilon_1 - \epsilon_0)} \mathbf{E}^{0^-}(\mathbf{u}). \quad (69)$$

This equation was already obtained with the extinction theorem.<sup>24</sup>

### B. A slab with a rough surface on the bottom side

We consider a slab delimited on the upper side by a planar surface and on the bottom side by a rough surface, see Fig. 4. Since there is no incident upward field in medium 2, the scattering matrix obtained in Sec. IV A is sufficient to determine the scattering matrix of the present configuration. In order to obtain proof, let us introduce some definitions as explained in Fig. 5. The scattering matrix for an incident plane wave coming from the medium 0, and scattered in the medium 1, is given by

$$\bar{\mathbf{V}}^0(\mathbf{p}|\mathbf{p}_0) = (2\pi)^2 \delta(\mathbf{p} - \mathbf{p}_0) \bar{\mathbf{V}}^{10}(\mathbf{p}_0), \quad (70)$$

where  $\bar{\mathbf{V}}^{10}$  is defined by Eq. (59). The transmitted waves in medium 1 are given by:

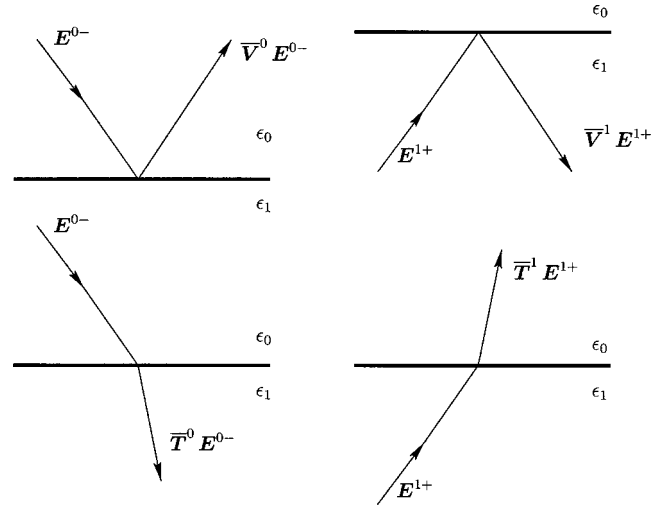


FIG. 5. Definitions of scattering matrices for a planar surface.

$$\bar{\mathbf{T}}^0(\mathbf{p}|\mathbf{p}_0) = (2\pi)^2 \delta(\mathbf{p} - \mathbf{p}_0) \frac{\alpha_0(\mathbf{p}_0)}{\alpha_1(\mathbf{p}_0)} \bar{\mathbf{T}}^{10}(\mathbf{p}_0), \quad (71)$$

$$\bar{\mathbf{T}}^{10}(\mathbf{p}_0) \equiv 2\alpha_1(\mathbf{p}_0) \begin{pmatrix} (\epsilon_0 \epsilon_1)^{1/2} & 0 \\ 0 & 1 \end{pmatrix} \cdot [\bar{\mathbf{D}}_{i0}^+(\mathbf{p}_0)]^{-1}. \quad (72)$$

Now, when the incident wave is coming from medium 1, we have, similarly,

$$\bar{\mathbf{V}}^1(\mathbf{p}|\mathbf{p}_0) = -(2\pi)^2 \delta(\mathbf{p} - \mathbf{p}_0) \bar{\mathbf{V}}^{10}(\mathbf{p}_0), \quad (73)$$

$$\bar{\mathbf{T}}^1(\mathbf{p}|\mathbf{p}_0) = (2\pi)^2 \delta(\mathbf{p} - \mathbf{p}_0) \bar{\mathbf{T}}^{10}(\mathbf{p}_0). \quad (74)$$

The scattering matrix  $\bar{\mathbf{R}}_{s\epsilon_1, \epsilon_2}^H$  for the rough surface  $h$ , which is located at  $z = -H$ ,<sup>30</sup> and separates two media of permittivity  $\epsilon_1$  and  $\epsilon_2$ , is given by

$$\bar{\mathbf{R}}_{s\epsilon_1, \epsilon_2}^H(\mathbf{p}|\mathbf{p}_0) = \exp\{i[\alpha_1(\mathbf{p}) + \alpha_1(\mathbf{p}_0)]H\} \bar{\mathbf{R}}_{s\epsilon_1, \epsilon_2}(\mathbf{p}|\mathbf{p}_0), \quad (75)$$

where the phase term comes from the translation  $z = -H$  [see Eq. (B2)], and  $\bar{\mathbf{R}}_{s\epsilon_1, \epsilon_2}$  denotes the scattering matrix  $\bar{\mathbf{R}}_{s\epsilon_0, \epsilon_1}$  of the Sec. IV A, where we have replaced  $\epsilon_0$  by  $\epsilon_1$  and  $\epsilon_1$  by  $\epsilon_2$ . Furthermore, if we define the product of two operator  $\bar{\mathbf{A}}$  and  $\bar{\mathbf{B}}$  by

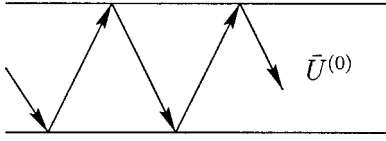
$$(\bar{\mathbf{A}} \cdot \bar{\mathbf{B}})(\mathbf{p}|\mathbf{p}_0) \equiv \int \frac{d^2 \mathbf{p}_1}{(2\pi)^2} \bar{\mathbf{A}}(\mathbf{p}|\mathbf{p}_1) \cdot \bar{\mathbf{B}}(\mathbf{p}_1|\mathbf{p}_0), \quad (76)$$

we can easily prove for the configuration shown in Fig. 4 that (we use for the fields the notations of Fig. 1),

$$\mathbf{E}^{1+} = \bar{\mathbf{R}}_{s\epsilon_1, \epsilon_2}^H \cdot \bar{\mathbf{T}}^0 \cdot \mathbf{E}^{0-} + \bar{\mathbf{R}}_{s\epsilon_1, \epsilon_2}^H \cdot \bar{\mathbf{V}}^1 \cdot \mathbf{E}^{1+}, \quad (77)$$

$$\mathbf{E}^{0+} = \bar{\mathbf{V}}^0 \cdot \mathbf{E}^{0-} + \bar{\mathbf{T}}^1 \cdot \mathbf{E}^{1+}, \quad (78)$$

where  $\mathbf{E}^{0-}(\mathbf{p}) = (2\pi)^2 \delta(\mathbf{p} - \mathbf{p}_0) \mathbf{E}^i(p_0)$ . These equations were recently used to calculate in first order the field scattered by a layered medium.<sup>14</sup> In fact, as we shall see below, these equations allow us to obtain all orders of the field perturbation. Expression (77) is analogous to the Dyson equation usually used in random media.<sup>4</sup> Thus we are naturally led to introduce a scattering operator  $\bar{\mathbf{U}}$ ,

FIG. 6. Diagrammatic representation of the operator  $\bar{\mathbf{U}}^{(0)}$ .

$$\mathbf{E}^{1+} = \bar{\mathbf{R}}_{s\epsilon_1, \epsilon_2}^H \cdot \bar{\mathbf{U}} \cdot \mathbf{T}^0 \cdot \bar{\mathbf{E}}^{0-}, \quad (79)$$

which satisfies the equation

$$\bar{\mathbf{U}} = \bar{\mathbf{I}} + \bar{\mathbf{V}}^1 \cdot \bar{\mathbf{R}}_{s\epsilon_1, \epsilon_2}^H \cdot \bar{\mathbf{U}}. \quad (80)$$

If we define by  $\bar{\mathbf{R}}_d(\mathbf{p}|\mathbf{p}_0)$ , the global scattering matrix for the upper planar surface and the bottom rough surface, by

$$\mathbf{E}^{0+}(\mathbf{p}) = \bar{\mathbf{R}}_d(\mathbf{p}|\mathbf{p}_0) \cdot \mathbf{E}^i(\mathbf{p}_0), \quad (81)$$

with Eqs. (78) and (79), the scattering matrix becomes

$$\bar{\mathbf{R}}_d = \bar{\mathbf{V}}^0 + \bar{\mathbf{T}}^1 \cdot \bar{\mathbf{R}}_{s\epsilon_1, \epsilon_2}^H \cdot \bar{\mathbf{U}} \cdot \bar{\mathbf{T}}^0. \quad (82)$$

We can improve development (80) by summing all the specular reflexions inside the slab; this can be done by introducing the operator  $\bar{\mathbf{U}}^{(0)}$  which satisfies the equation

$$\bar{\mathbf{U}}^{(0)} = \bar{\mathbf{I}} + \bar{\mathbf{V}}^1 \cdot \bar{\mathbf{R}}_{s\epsilon_1, \epsilon_2}^{H(0)} \cdot \bar{\mathbf{U}}^{(0)}, \quad (83)$$

where  $\bar{\mathbf{R}}_{s\epsilon_1, \epsilon_2}^{H(0)}$  is the zeroth-order term of the perturbative development, which is given by

$$\bar{\mathbf{R}}_{s\epsilon_1, \epsilon_2}^{H(0)}(\mathbf{p}|\mathbf{p}_0) = (2\pi)^2 \delta(\mathbf{p} - \mathbf{p}_0) \bar{\mathbf{V}}^{H21}(\mathbf{p}_0), \quad (84)$$

and,  $\bar{\mathbf{V}}^{H21}$  is the scattering matrix for a planar surface located at the height  $z = -H$ :

$$\bar{\mathbf{V}}^{H21}(\mathbf{u}) \equiv \exp[2i\alpha_1(\mathbf{u})H] \bar{\mathbf{D}}_{21}^-(\mathbf{p}_0) \cdot [\bar{\mathbf{D}}_{21}^+(\mathbf{p}_0)]^{-1}, \quad (85)$$

$$\bar{\mathbf{D}}_{21}^\pm(\mathbf{p}_0) \equiv \begin{pmatrix} \epsilon_2 \alpha_1(\mathbf{p}_0) \pm \epsilon_1 \alpha_2(\mathbf{p}_0) & 0 \\ 0 & \alpha_1(\mathbf{p}_0) \pm \alpha_2(\mathbf{p}_0) \end{pmatrix}. \quad (86)$$

The term  $\exp[2i\alpha_1(\mathbf{u})H]$  comes from the phase shift induced by the translation of the planar surface from the height  $z = 0$  to  $z = -H$  [see Eq. (B2)]. The diagrammatic representation of Eq. (83), shown in Fig. 6, is in fact a geometric series

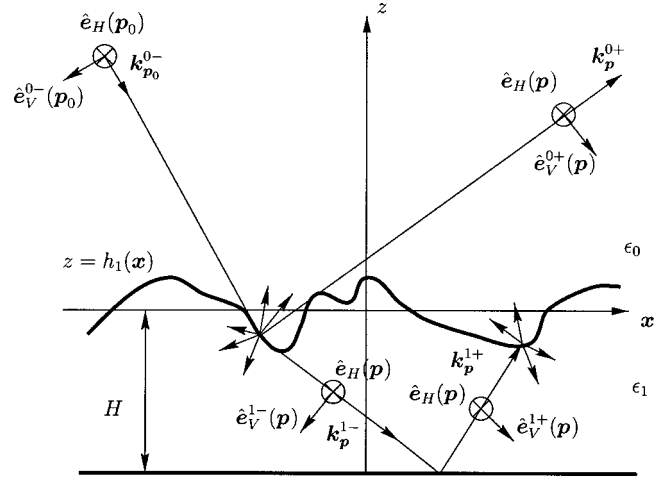


FIG. 7. A slab formed with an upper two-dimensional rough surface and a bottom planar surface.

which can be summed as

$$\bar{\mathbf{U}}^{(0)}(\mathbf{p}|\mathbf{p}_0) = (2\pi)^2 \delta(\mathbf{p} - \mathbf{p}_0) \bar{\mathbf{U}}^{(0)}(\mathbf{p}_0), \quad (87)$$

$$\bar{\mathbf{U}}^{(0)}(\mathbf{p}_0) \equiv [\bar{\mathbf{I}} + \bar{\mathbf{V}}^{10}(\mathbf{p}_0) \cdot \bar{\mathbf{V}}^{H21}(\mathbf{p}_0)]^{-1}. \quad (88)$$

From the previous results, Eq. (80) can be written in the form

$$\bar{\mathbf{U}} = \bar{\mathbf{U}}^{(0)} + \bar{\mathbf{U}}^{(0)} \cdot \bar{\mathbf{V}}^1 \cdot \Delta \bar{\mathbf{R}}_{s\epsilon_1, \epsilon_2}^H \cdot \bar{\mathbf{U}}, \quad (89)$$

where

$$\Delta \bar{\mathbf{R}}_{s\epsilon_1, \epsilon_2}^H \equiv \bar{\mathbf{R}}_{s\epsilon_1, \epsilon_2}^H - \bar{\mathbf{R}}_{s\epsilon_1, \epsilon_2}^{H(0)}. \quad (90)$$

In order to obtain the perturbative development of  $\bar{\mathbf{R}}_d$ , we introduce the expansion

$$\bar{\mathbf{R}}_{s\epsilon_1, \epsilon_2}^H = \bar{\mathbf{R}}_{s\epsilon_1, \epsilon_2}^{H(0)} + \bar{\mathbf{R}}_{s\epsilon_1, \epsilon_2}^{H(1)} + \bar{\mathbf{R}}_{s\epsilon_1, \epsilon_2}^{H(2)} + \bar{\mathbf{R}}_{s\epsilon_1, \epsilon_2}^{H(3)}, \quad (91)$$

in Eqs. (82) and (89), which gives the following terms:

$$\bar{\mathbf{R}}_d^{(0)} = \bar{\mathbf{V}}^0 + \bar{\mathbf{T}}^1 \cdot \bar{\mathbf{R}}_{s\epsilon_1, \epsilon_2}^{H(0)} \cdot \bar{\mathbf{U}}^{(0)} \cdot \bar{\mathbf{T}}^0, \quad (92)$$

$$\bar{\mathbf{R}}_d^{(1)} = \bar{\mathbf{T}}^1 \cdot \bar{\mathbf{U}}^{(0)} \cdot \bar{\mathbf{R}}_{s\epsilon_1, \epsilon_2}^{H(1)} \cdot \bar{\mathbf{U}}^{(0)} \cdot \bar{\mathbf{T}}^0, \quad (93)$$

$$\bar{\mathbf{R}}_d^{(2)} = \bar{\mathbf{T}}^1 \cdot \bar{\mathbf{U}}^{(0)} \cdot [\bar{\mathbf{R}}_{s\epsilon_1, \epsilon_2}^{H(2)} + \bar{\mathbf{R}}_{s\epsilon_1, \epsilon_2}^{H(1)} \cdot \bar{\mathbf{U}}^{(0)} \cdot \bar{\mathbf{V}}^1 \cdot \bar{\mathbf{R}}_{s\epsilon_1, \epsilon_2}^{H(1)}] \cdot \bar{\mathbf{U}}^{(0)} \cdot \bar{\mathbf{T}}^0, \quad (94)$$

$$\begin{aligned} \bar{\mathbf{R}}_d^{(3)} = & \bar{\mathbf{T}}^1 \cdot \bar{\mathbf{U}}^{(0)} \cdot [\bar{\mathbf{R}}_{s\epsilon_1, \epsilon_2}^{H(3)} + \bar{\mathbf{R}}_{s\epsilon_1, \epsilon_2}^{H(2)} \cdot \bar{\mathbf{U}}^{(0)} \cdot \bar{\mathbf{V}}^1 \cdot \bar{\mathbf{R}}_{s\epsilon_1, \epsilon_2}^{H(1)} + \bar{\mathbf{R}}_{s\epsilon_1, \epsilon_2}^{H(1)} \cdot \bar{\mathbf{U}}^{(0)} \cdot \bar{\mathbf{V}}^1 \cdot \bar{\mathbf{R}}_{s\epsilon_1, \epsilon_2}^{H(2)} \\ & + \bar{\mathbf{R}}_{s\epsilon_1, \epsilon_2}^{H(1)} \cdot \bar{\mathbf{U}}^{(0)} \cdot \bar{\mathbf{V}}^1 \cdot \bar{\mathbf{R}}_{s\epsilon_1, \epsilon_2}^{H(1)} \cdot \bar{\mathbf{U}}^{(0)} \cdot \bar{\mathbf{V}}^1 \cdot \bar{\mathbf{R}}_{s\epsilon_1, \epsilon_2}^{H(1)}] \cdot \bar{\mathbf{U}}^{(0)} \cdot \bar{\mathbf{T}}^0. \end{aligned} \quad (95)$$

Using development (53) for  $\bar{\mathbf{R}}_{s\epsilon_1, \epsilon_2}^H$ , and definitions (70), (71), (73), and (74), we obtain, after some calculation a development of the form of Eq. (53) for  $\bar{\mathbf{R}}_d$  with the following coefficients:

$$\bar{\mathbf{X}}_d^{(0)}(\mathbf{p}_0) = [\bar{\mathbf{V}}^{10}(\mathbf{p}_0) + \bar{\mathbf{V}}^{H21}(\mathbf{p}_0)] \cdot [\bar{\mathbf{I}} + \bar{\mathbf{V}}^{10}(\mathbf{p}_0) \cdot \bar{\mathbf{V}}^{H21}(\mathbf{p}_0)]^{-1}. \quad (96)$$

This matrix is naturally diagonal, and its coefficients are identical to those of the reflection coefficients for a planar slab.<sup>4</sup> The other coefficients are

$$\bar{\mathbf{X}}_d^{(1)}(\mathbf{p}|\mathbf{p}_0) = \bar{\mathbf{T}}^{10}(\mathbf{p}) \cdot \bar{\mathbf{U}}^{(0)}(\mathbf{p}) \cdot \bar{\mathbf{X}}_{s\epsilon_1, \epsilon_2}^{H(1)}(\mathbf{p}|\mathbf{p}_0) \cdot \bar{\mathbf{U}}^{(0)}(\mathbf{p}_0) \cdot \bar{\mathbf{T}}^{10}(\mathbf{p}_0), \quad (97)$$

$$\begin{aligned} \bar{\mathbf{X}}_d^{(2)}(\mathbf{p}|\mathbf{p}_1|\mathbf{p}_0) &= \bar{\mathbf{T}}^{10}(\mathbf{p}) \cdot \bar{\mathbf{U}}^{(0)}(\mathbf{p}) \cdot [\bar{\mathbf{X}}_{s\epsilon_1, \epsilon_2}^{H(2)}(\mathbf{p}|\mathbf{p}_1|\mathbf{p}_0) - \alpha_1(\mathbf{p}_1) \bar{\mathbf{X}}_{s\epsilon_1, \epsilon_2}^{H(1)}(\mathbf{p}|\mathbf{p}_1) \cdot \bar{\mathbf{U}}^{(0)}(\mathbf{p}_1) \cdot \bar{\mathbf{V}}^{10}(\mathbf{p}_1) \cdot \bar{\mathbf{X}}_{s\epsilon_1, \epsilon_2}^{H(1)}(\mathbf{p}_1|\mathbf{p}_0)] \\ &\quad \cdot \bar{\mathbf{U}}^{(0)}(\mathbf{p}_0) \cdot \bar{\mathbf{T}}^{10}(\mathbf{p}_0), \end{aligned} \quad (98)$$

$$\begin{aligned} \bar{\mathbf{X}}_d^{(3)}(\mathbf{p}|\mathbf{p}_1|\mathbf{p}_2|\mathbf{p}_0) &= \bar{\mathbf{T}}^{10}(\mathbf{p}) \cdot \bar{\mathbf{U}}^{(0)}(\mathbf{p}) \cdot [\bar{\mathbf{X}}_{s\epsilon_1, \epsilon_2}^{H(3)}(\mathbf{p}|\mathbf{p}_1|\mathbf{p}_2|\mathbf{p}_0) - \alpha_1(\mathbf{p}_2) \bar{\mathbf{X}}_{s\epsilon_1, \epsilon_2}^{H(2)}(\mathbf{p}|\mathbf{p}_1|\mathbf{p}_2) \cdot \bar{\mathbf{U}}^{(0)}(\mathbf{p}_2) \cdot \bar{\mathbf{V}}^{10}(\mathbf{p}_2) \cdot \bar{\mathbf{X}}_{s\epsilon_1, \epsilon_2}^{H(1)}(\mathbf{p}_2|\mathbf{p}_0) \\ &\quad - \alpha_1(\mathbf{p}_1) \bar{\mathbf{X}}_{s\epsilon_1, \epsilon_2}^{H(1)}(\mathbf{p}|\mathbf{p}_1) \cdot \bar{\mathbf{U}}^{(0)}(\mathbf{p}_1) \cdot \bar{\mathbf{V}}^{10}(\mathbf{p}_1) \cdot \bar{\mathbf{X}}_{s\epsilon_1, \epsilon_2}^{H(2)}(\mathbf{p}_1|\mathbf{p}_2|\mathbf{p}_0) + \alpha_1(\mathbf{p}_1) \alpha_1(\mathbf{p}_2) \bar{\mathbf{X}}_{s\epsilon_1, \epsilon_2}^{H(1)}(\mathbf{p}|\mathbf{p}_1) \\ &\quad \cdot \bar{\mathbf{U}}^{(0)}(\mathbf{p}_1) \cdot \bar{\mathbf{V}}^{10}(\mathbf{p}_1) \cdot \bar{\mathbf{X}}_{s\epsilon_1, \epsilon_2}^{H(1)}(\mathbf{p}_1|\mathbf{p}_2) \cdot \bar{\mathbf{U}}^{(0)}(\mathbf{p}_2) \cdot \bar{\mathbf{V}}^{10}(\mathbf{p}_2) \cdot \bar{\mathbf{X}}_{s\epsilon_1, \epsilon_2}^{H(1)}(\mathbf{p}_2|\mathbf{p}_0)] \cdot \bar{\mathbf{U}}^{(0)}(\mathbf{p}_0) \cdot \bar{\mathbf{T}}^{10}(\mathbf{p}_0). \end{aligned} \quad (99)$$

In these expressions,  $\bar{\mathbf{X}}_{s\epsilon_1, \epsilon_2}^{H(n)}(\mathbf{p}|\mathbf{p}_0) \equiv \exp\{i[\alpha_1(\mathbf{p}) + \alpha_1(\mathbf{p}_0)]H\} \bar{\mathbf{X}}_{s\epsilon_1, \epsilon_2}^{(n)}(\mathbf{p}|\mathbf{p}_0)$ , and the subscripts  $\epsilon_1$  and  $\epsilon_2$  in  $\bar{\mathbf{X}}_{s\epsilon_1, \epsilon_2}$  mean that we replace  $\epsilon_0$  by  $\epsilon_1$ , and  $\epsilon_1$  by  $\epsilon_2$  in Eqs. (61)–(63).

### C. A slab with a rough surface on the upper side

We consider a slab delimited on the upper side by a two-dimensional rough surface, and on the bottom side by a planar surface; see Fig. 7. To derive the reduced Rayleigh equation for this configuration, we have to combine the equations

$$\int \frac{d^2\mathbf{p}}{(2\pi)^2} \bar{\mathbf{M}}_h^{1+,0+}(\mathbf{u}|\mathbf{p}) \cdot \bar{\mathbf{R}}_u(\mathbf{p}|\mathbf{p}_0) \cdot \mathbf{E}^i(\mathbf{p}_0) + \bar{\mathbf{M}}_h^{1+,0-}(\mathbf{u}|\mathbf{p}_0) \cdot \mathbf{E}^i(\mathbf{p}_0) = \frac{2(\epsilon_0\epsilon_1)^{1/2}\alpha_1(\mathbf{u})}{(\epsilon_1 - \epsilon_0)} \mathbf{E}^{1+}(\mathbf{u}), \quad (100)$$

$$\int \frac{d^2\mathbf{p}}{(2\pi)^2} \bar{\mathbf{M}}_h^{1-,0+}(\mathbf{u}|\mathbf{p}) \cdot \bar{\mathbf{R}}_u(\mathbf{p}|\mathbf{p}_0) \cdot \mathbf{E}^i(\mathbf{p}_0) + \bar{\mathbf{M}}_h^{1-,0-}(\mathbf{u}|\mathbf{p}_0) \cdot \mathbf{E}^i(\mathbf{p}_0) = -\frac{2(\epsilon_0\epsilon_1)^{1/2}\alpha_1(\mathbf{u})}{(\epsilon_1 - \epsilon_0)} \mathbf{E}^{1-}(\mathbf{u}), \quad (101)$$

with

$$\mathbf{E}^{1+}(\mathbf{u}) = \bar{\mathbf{V}}^{H\ 21}(\mathbf{u}) \cdot \mathbf{E}^{1-}(\mathbf{u}), \quad (102)$$

where  $\bar{\mathbf{V}}^{H\ 21}$  is given by Eq. (86), and  $\bar{\mathbf{R}}_u$  is the global scattering matrix for the upper rough surface and the bottom planar surface.

The reduced Rayleigh equation for the scattering matrix  $\bar{\mathbf{R}}_u$  is then

$$\int \frac{d^2\mathbf{p}}{(2\pi)^2} [\bar{\mathbf{M}}_h^{1+,0+}(\mathbf{u}|\mathbf{p}) + \bar{\mathbf{V}}^{H\ 21}(\mathbf{u}) \cdot \bar{\mathbf{M}}_h^{1-,0+}(\mathbf{u}|\mathbf{p})] \cdot \bar{\mathbf{R}}_u(\mathbf{p}|\mathbf{p}_0) = -[\bar{\mathbf{M}}_h^{1+,0-}(\mathbf{u}|\mathbf{p}_0) + \bar{\mathbf{V}}^{H\ 21}(\mathbf{u}) \cdot \bar{\mathbf{M}}_h^{1-,0-}(\mathbf{u}|\mathbf{p}_0)]. \quad (103)$$

With the expansion of  $I(\alpha|\mathbf{p})$  in a power series, we obtain the perturbative development

$$\begin{aligned} \bar{\mathbf{X}}_u^{(0)}(\mathbf{p}_0) &= -\left[ \frac{\bar{\mathbf{M}}_h^{1+,0+}(\mathbf{p}_0|\mathbf{p}_0)}{\alpha_1(\mathbf{p}_0) - \alpha_0(\mathbf{p}_0)} - \bar{\mathbf{V}}^{H\ 21}(\mathbf{p}_0) \frac{\bar{\mathbf{M}}_h^{1-,0+}(\mathbf{p}_0|\mathbf{p}_0)}{\alpha_1(\mathbf{p}_0) + \alpha_0(\mathbf{p}_0)} \right]^{-1} \cdot \left[ \frac{\bar{\mathbf{M}}_h^{1+,0-}(\mathbf{p}_0|\mathbf{p}_0)}{\alpha_1(\mathbf{p}_0) + \alpha_0(\mathbf{p}_0)} + \bar{\mathbf{V}}^{H\ 21}(\mathbf{p}_0) \cdot \frac{\bar{\mathbf{M}}_h^{1-,0-}(\mathbf{p}_0|\mathbf{p}_0)}{-\alpha_1(\mathbf{p}_0) + \alpha_0(\mathbf{p}_0)} \right] \\ &= [\bar{\mathbf{V}}^{10}(\mathbf{p}_0) + \bar{\mathbf{V}}^{H\ 21}(\mathbf{p}_0)] \cdot [\bar{\mathbf{I}} + \bar{\mathbf{V}}^{10}(\mathbf{p}_0) \cdot \bar{\mathbf{V}}^{H\ 21}(\mathbf{p}_0)]^{-1}, \end{aligned} \quad (104)$$

$$\bar{\mathbf{X}}_u^{(1)}(\mathbf{u}|\mathbf{p}_0) \equiv 2i\bar{\mathbf{Q}}^{++}(\mathbf{u}|\mathbf{p}_0) \quad (105)$$

$$\bar{\mathbf{X}}_u^{(2)}(\mathbf{u}|\mathbf{p}_1|\mathbf{p}_0) = \alpha_1(\mathbf{u})\bar{\mathbf{Q}}^{-+}(\mathbf{u}|\mathbf{p}_0) + \alpha_0(\mathbf{p}_0)\bar{\mathbf{Q}}^{+-}(\mathbf{u}|\mathbf{p}_0) - 2\bar{\mathbf{P}}^+(\mathbf{u}|\mathbf{p}_1) \cdot \bar{\mathbf{Q}}^{++}(\mathbf{p}_1|\mathbf{p}_0) \quad (106)$$

$$\begin{aligned} \bar{\mathbf{X}}_u^{(3)}(\mathbf{u}|\mathbf{p}_1|\mathbf{p}_2|\mathbf{p}_0) &= -\frac{i}{3} \{ [\alpha_1^2(\mathbf{u}) + \alpha_0^2(\mathbf{p}_0)] \bar{\mathbf{Q}}^{++}(\mathbf{u}|\mathbf{p}_0) + 2\alpha_1(\mathbf{u})\alpha_0(\mathbf{p}_0)\bar{\mathbf{Q}}^{--}(\mathbf{u}|\mathbf{p}_0) \} + i\bar{\mathbf{P}}^+(\mathbf{u}|\mathbf{p}_1) \cdot \bar{\mathbf{X}}^{(2)}(\mathbf{p}_1|\mathbf{p}_2|\mathbf{p}_0) \\ &\quad + i[\alpha_1(\mathbf{u})\bar{\mathbf{P}}^-(\mathbf{u}|\mathbf{p}_2) - \alpha_0(\mathbf{p}_2)\bar{\mathbf{P}}^+(\mathbf{u}|\mathbf{p}_2)] \cdot \bar{\mathbf{Q}}^{++}(\mathbf{p}_2|\mathbf{p}_0) \end{aligned} \quad (107)$$

with

$$\begin{aligned} \bar{\mathbf{Q}}^{ba}(\mathbf{u}|\mathbf{p}_0) &\equiv \frac{1}{2\alpha_0(\mathbf{p}_0)} \left[ \frac{\bar{\mathbf{M}}_h^{1+,0+}(\mathbf{u}|\mathbf{u})}{\alpha_1(\mathbf{u}) - \alpha_0(\mathbf{u})} - \bar{\mathbf{V}}^{H\ 21}(\mathbf{u}) \cdot \frac{\bar{\mathbf{M}}_h^{1-,0+}(\mathbf{u}|\mathbf{u})}{\alpha_1(\mathbf{u}) + \alpha_0(\mathbf{u})} \right]^{-1} \cdot [a\bar{\mathbf{M}}_h^{1+,0+}(\mathbf{u}|\mathbf{p}_0) \cdot \bar{\mathbf{X}}_{s\epsilon_0, \epsilon_1}^{(0)}(\mathbf{p}_0) + \bar{\mathbf{M}}_h^{1+,0-}(\mathbf{u}|\mathbf{p}_0) \\ &\quad + b\bar{\mathbf{V}}^{H\ 21}(\mathbf{u}) \cdot [a\bar{\mathbf{M}}_h^{1-,0+}(\mathbf{u}|\mathbf{p}_0) \cdot \bar{\mathbf{X}}_{s\epsilon_0, \epsilon_1}^{(0)}(\mathbf{p}_0) + \bar{\mathbf{M}}_h^{1-,0-}(\mathbf{u}|\mathbf{p}_0)]], \end{aligned} \quad (108)$$

$$\bar{\mathbf{P}}^\pm(\mathbf{u}|\mathbf{p}_1) \equiv \left[ \frac{\bar{\mathbf{M}}_h^{1+,0+}(\mathbf{u}|\mathbf{u})}{\alpha_1(\mathbf{u}) - \alpha_0(\mathbf{u})} - \bar{\mathbf{V}}^{H\ 21}(\mathbf{u}) \cdot \frac{\bar{\mathbf{M}}_h^{1-,0+}(\mathbf{u}|\mathbf{u})}{\alpha_1(\mathbf{u}) + \alpha_0(\mathbf{u})} \right]^{-1} \cdot [\bar{\mathbf{M}}_h^{1+,0+}(\mathbf{u}|\mathbf{p}_1) \pm \bar{\mathbf{V}}^{H\ 21}(\mathbf{u}) \cdot \bar{\mathbf{M}}_h^{1-,0+}(\mathbf{u}|\mathbf{p}_1)], \quad (109)$$

where,  $a = \pm$  and  $b = \pm$  are the sign indices. After some computations we obtain

$$\bar{\mathbf{Q}}^{++}(\mathbf{u}|\mathbf{p}_0) = (\epsilon_1 - \epsilon_0)[\bar{\mathbf{D}}_{10}^+(\mathbf{u})]^{-1} \cdot \begin{pmatrix} \epsilon_1 \|\mathbf{u}\| \|\mathbf{p}_0\| F_V^+(\mathbf{u}) F_V^+(\mathbf{p}_0) - \epsilon_0 \alpha_1(\mathbf{u}) \alpha_1(\mathbf{p}_0) F_V^-(\mathbf{u}) F_V^-(\mathbf{p}_0) \hat{\mathbf{u}} \cdot \hat{\mathbf{p}}_0 & -\epsilon_0^{1/2} K_0 \alpha_1(\mathbf{u}) F_V^-(\mathbf{u}) F_H^+(\mathbf{p}_0) (\hat{\mathbf{u}} \times \hat{\mathbf{p}}_0)_z \\ -\epsilon_0^{1/2} K_0 \alpha_1(\mathbf{p}_0) F_H^+(\mathbf{u}) F_V^-(\mathbf{p}_0) (\hat{\mathbf{u}} \times \hat{\mathbf{p}}_0)_z & K_0^2 F_H^+(\mathbf{u}) F_H^+(\mathbf{p}_0) \hat{\mathbf{u}} \cdot \hat{\mathbf{p}}_0 \end{pmatrix} \cdot [\bar{\mathbf{D}}_{10}^+(\mathbf{p}_0)]^{-1}, \quad (110)$$

$$\bar{\mathbf{Q}}^{-+}(\mathbf{u}|\mathbf{p}_0) = (\epsilon_1 - \epsilon_0)[\bar{\mathbf{D}}_{10}^+(\mathbf{u})]^{-1} \cdot \begin{pmatrix} \epsilon_1 \|\mathbf{u}\| \|\mathbf{p}_0\| F_V^-(\mathbf{u}) F_V^+(\mathbf{p}_0) - \epsilon_0 \alpha_1(\mathbf{u}) \alpha_1(\mathbf{p}_0) F_V^+(\mathbf{u}) F_V^-(\mathbf{p}_0) \hat{\mathbf{u}} \cdot \hat{\mathbf{p}}_0 & -\epsilon_0^{1/2} K_0 \alpha_1(\mathbf{u}) F_V^+(\mathbf{u}) F_H^+(\mathbf{p}_0) (\hat{\mathbf{u}} \times \hat{\mathbf{p}}_0)_z \\ -\epsilon_0^{1/2} K_0 \alpha_1(\mathbf{p}_0) F_H^-(\mathbf{u}) F_V^-(\mathbf{p}_0) (\hat{\mathbf{u}} \times \hat{\mathbf{p}}_0)_z & K_0^2 F_H^-(\mathbf{u}) F_H^+(\mathbf{p}_0) \hat{\mathbf{u}} \cdot \hat{\mathbf{p}}_0 \end{pmatrix} \cdot [\bar{\mathbf{D}}_{10}^+(\mathbf{p}_0)]^{-1}, \quad (111)$$

$$\bar{\mathbf{Q}}^{+-}(\mathbf{u}|\mathbf{p}_0) = \frac{(\epsilon_1 - \epsilon_0)}{\alpha_0(p_0)} [\bar{\mathbf{D}}_{10}^+(\mathbf{u})]^{-1} \cdot \begin{pmatrix} \epsilon_0 \alpha_1(\mathbf{p}_0) \|\mathbf{u}\| \|\mathbf{p}_0\| F_V^+(\mathbf{u}) F_V^-(\mathbf{p}_0) - \epsilon_1 \alpha_1(\mathbf{u}) \alpha_0^2(\mathbf{p}_0) F_V^-(\mathbf{u}) F_V^+(\mathbf{p}_0) \hat{\mathbf{u}} \cdot \hat{\mathbf{p}}_0 & -\epsilon_0^{1/2} K_0 \alpha_1(\mathbf{u}) \alpha_1(\mathbf{p}_0) F_V^-(\mathbf{u}) F_H^-(\mathbf{p}_0) (\hat{\mathbf{u}} \times \hat{\mathbf{p}}_0)_z \\ -\epsilon_0^{-1/2} \epsilon_1 K_0 \alpha_0^2(\mathbf{p}_0) F_H^+(\mathbf{u}) F_V^+(\mathbf{p}_0) (\hat{\mathbf{u}} \times \hat{\mathbf{p}}_0)_z & K_0^2 \alpha_1(\mathbf{p}_0) F_H^+(\mathbf{u}) F_H^-(\mathbf{p}_0) \hat{\mathbf{u}} \cdot \hat{\mathbf{p}}_0 \end{pmatrix} \cdot [\bar{\mathbf{D}}_{10}^+(\mathbf{p}_0)]^{-1}, \quad (112)$$

$$\bar{\mathbf{Q}}^{--}(\mathbf{u}|\mathbf{p}_0) = \frac{(\epsilon_1 - \epsilon_0)}{\alpha_0(p_0)} [\bar{\mathbf{D}}_{10}^+(\mathbf{u})]^{-1} \cdot \begin{pmatrix} \epsilon_0 \alpha_1(\mathbf{p}_0) \|\mathbf{u}\| \|\mathbf{p}_0\| F_V^-(\mathbf{u}) F_V^-(\mathbf{p}_0) - \epsilon_1 \alpha_1(\mathbf{u}) \alpha_0^2(\mathbf{p}_0) F_V^+(\mathbf{u}) F_V^+(\mathbf{p}_0) \hat{\mathbf{u}} \cdot \hat{\mathbf{p}}_0 & -\epsilon_0^{1/2} K_0 \alpha_1(\mathbf{u}) \alpha_1(\mathbf{p}_0) F_V^+(\mathbf{u}) F_H^-(\mathbf{p}_0) (\hat{\mathbf{u}} \times \hat{\mathbf{p}}_0)_z \\ -\epsilon_0^{-1/2} \epsilon_1 K_0 \alpha_0^2(\mathbf{p}_0) F_H^-(\mathbf{u}) F_V^+(\mathbf{p}_0) (\hat{\mathbf{u}} \times \hat{\mathbf{p}}_0)_z & K_0^2 \alpha_1(\mathbf{p}_0) F_H^-(\mathbf{u}) F_H^-(\mathbf{p}_0) \hat{\mathbf{u}} \cdot \hat{\mathbf{p}}_0 \end{pmatrix} \cdot [\bar{\mathbf{D}}_{10}^+(\mathbf{p}_0)]^{-1}, \quad (113)$$

where

$$\begin{pmatrix} F_V^\pm(\mathbf{p}_0) & 0 \\ 0 & F_H^\pm(\mathbf{p}_0) \end{pmatrix} = [\bar{\mathbf{I}} \pm \bar{\mathbf{V}}^{H^{21}}(\mathbf{p}_0)] \cdot [\bar{\mathbf{I}} + \bar{\mathbf{V}}^{10}(\mathbf{p}_0) \cdot \bar{\mathbf{V}}^{H^{21}}(\mathbf{p}_0)]^{-1} \quad (114)$$

and

$$\bar{\mathbf{P}}^+(\mathbf{u}|\mathbf{p}_1) = (\epsilon_1 - \epsilon_0)[\bar{\mathbf{D}}_{10}^+(\mathbf{u})]^{-1} \cdot \begin{pmatrix} \|\mathbf{u}\| \|\mathbf{p}_1\| F_V^+(\mathbf{u}) + \alpha_1(\mathbf{u}) \alpha_0(\mathbf{p}_1) F_V^-(\mathbf{u}) \hat{\mathbf{u}} \cdot \hat{\mathbf{p}}_1 & -\epsilon_0^{1/2} K_0 \alpha_1(\mathbf{u}) F_V^-(\mathbf{u}) (\hat{\mathbf{u}} \times \hat{\mathbf{p}}_1)_z \\ \epsilon_0^{-1/2} K_0 \alpha_0(\mathbf{p}_1) F_H^+(\mathbf{u}) (\hat{\mathbf{u}} \times \hat{\mathbf{p}}_1)_z & K_0^2 F_H^+(\mathbf{u}) \hat{\mathbf{u}} \cdot \hat{\mathbf{p}}_1 \end{pmatrix}, \quad (115)$$

$$\bar{\mathbf{P}}^-(\mathbf{u}|\mathbf{p}_1) = (\epsilon_1 - \epsilon_0)[\bar{\mathbf{D}}_{10}^+(\mathbf{u})]^{-1} \cdot \begin{pmatrix} \|\mathbf{u}\| \|\mathbf{p}_1\| F_V^-(\mathbf{u}) + \alpha_1(\mathbf{u}) \alpha_0(\mathbf{p}_1) F_V^+(\mathbf{u}) \hat{\mathbf{u}} \cdot \hat{\mathbf{p}}_1 & -\epsilon_0^{1/2} K_0 \alpha_1(\mathbf{u}) F_V^+(\mathbf{u}) (\hat{\mathbf{u}} \times \hat{\mathbf{p}}_1)_z \\ \epsilon_0^{-1/2} K_0 \alpha_0(\mathbf{p}_1) F_H^-(\mathbf{u}) (\hat{\mathbf{u}} \times \hat{\mathbf{p}}_1)_z & K_0^2 F_H^-(\mathbf{u}) \hat{\mathbf{u}} \cdot \hat{\mathbf{p}}_1 \end{pmatrix}. \quad (116)$$

The first-order term was recently derived in Ref. 14. They noted that, for this order, the matrix differs from the one obtained for a surface separating two semi-infinite media by only the factors  $F^\pm$ . Likewise, for higher order, we see that Eqs. (110) and (111) differ from Eq. (66) by only  $F^\pm$ , and similarly for Eqs. (112) and (113) with respect to Eq. (67), and Eqs. (115) and (116) with respect to Eq. (68). So when the thickness  $H$  becomes infinite, and the absorption  $\text{Im}(\epsilon_1) \neq 0$ , or  $\epsilon_1 = \epsilon_2$ , we have  $\bar{\mathbf{V}}^{H \rightarrow \infty} = 0$ ; thus  $F^\pm = 1$ , and in this case we recover the matrix equations (66)–(68) for a rough surface between two semi-infinite media.

## V. MUELLER MATRIX CROSS SECTION AND SURFACE STATISTIC

When we consider an observation point in the far-field limit, the saddle-point method gives an asymptotic form for the scattered field  $\mathbf{E}^s \equiv \mathbf{E}^{0+}$  obtained from Eq. (51):

$$\mathbf{E}^s(\mathbf{x}, z) = \frac{\exp(iK_0 \|\mathbf{r}\|)}{\|\mathbf{r}\|} \bar{\mathbf{f}}(\mathbf{p}|\mathbf{p}_0) \cdot \mathbf{E}^i(\mathbf{p}_0), \quad (117)$$

with

$$\bar{\mathbf{f}}(\mathbf{p}|\mathbf{p}_0) \equiv \frac{K_0 \cos \theta}{2\pi i} \bar{\mathbf{R}}(\mathbf{p}|\mathbf{p}_0) \quad (118)$$

$$\mathbf{p} = K_0 \frac{\mathbf{x}}{\|\mathbf{r}\|}, \quad (119)$$

where  $\theta$  is the angle between  $\hat{\mathbf{e}}_z$  and the scattering direction (see Fig. 2). In order to describe the incident and the scattered waves, we introduce the modified Stokes parameters

$$\mathbf{I}^s(\mathbf{p}) \equiv \begin{pmatrix} |E_V^s(\mathbf{p})|^2 \\ |E_H^s(\mathbf{p})|^2 \\ 2 \text{Re}[E_V^s(\mathbf{p})E_H^s(\mathbf{p})] \\ 2 \text{Im}[E_V^s(\mathbf{p})E_H^s(\mathbf{p})] \end{pmatrix},$$

$$\mathbf{I}^i(\mathbf{p}_0) \equiv \begin{pmatrix} |E_V^i(\mathbf{p}_0)|^2 \\ |E_H^i(\mathbf{p}_0)|^2 \\ 2 \text{Re}[E_V^i(\mathbf{p}_0)E_H^i(\mathbf{p}_0)] \\ 2 \text{Im}[E_V^i(\mathbf{p}_0)E_H^i(\mathbf{p}_0)] \end{pmatrix}. \quad (120)$$

The analog of the scattering matrix for these parameters is the Mueller matrix, defined<sup>2</sup> by

$$\mathbf{I}^s(\mathbf{p}) \equiv \frac{1}{\|\mathbf{r}\|^2} \bar{\mathbf{M}}(\mathbf{p}|\mathbf{p}_0) \cdot \mathbf{I}^i(\mathbf{p}_0), \quad (121)$$

which can be expressed as a function<sup>2</sup> of  $\bar{\mathbf{f}}(\mathbf{p}|\mathbf{p}_0)$ . To maintain a matrix formulation in the following calculations, we introduce a product between two-dimensional matrices with the definition

$$\bar{\mathbf{f}} \odot \bar{\mathbf{g}} \equiv \begin{pmatrix} f_{VV} & f_{VH} \\ f_{HV} & f_{HH} \end{pmatrix} \odot \begin{pmatrix} g_{VV} & g_{VH} \\ g_{HV} & g_{HH} \end{pmatrix}$$

$$= \begin{pmatrix} f_{VV}g_{VV}^* & f_{VH}g_{VH}^* & \text{Re}(f_{VV}g_{VH}^*) & -\text{Im}(f_{VV}g_{VH}^*) \\ f_{HV}g_{HV}^* & f_{HH}g_{HH}^* & \text{Re}(f_{HV}g_{HH}^*) & -\text{Im}(f_{HV}g_{HH}^*) \\ 2 \text{Re}(f_{VV}g_{HV}^*) & 2 \text{Re}(f_{VH}g_{HH}^*) & \text{Re}(f_{VV}g_{VV}^* + f_{HV}g_{VH}^*) & -\text{Im}(f_{VV}g_{HH}^* - f_{VH}g_{HV}^*) \\ 2 \text{Im}(f_{VV}g_{HV}^*) & 2 \text{Im}(f_{VH}g_{HH}^*) & \text{Im}(f_{VV}g_{VV}^* + f_{HV}g_{VH}^*) & \text{Re}(f_{VV}g_{HH}^* - f_{VH}g_{HV}^*) \end{pmatrix}. \quad (122)$$

This product allows one to express the matrix  $\bar{\mathbf{M}}$  as

$$\bar{\mathbf{M}}(\mathbf{p}|\mathbf{p}_0) = \bar{\mathbf{f}}(\mathbf{p}|\mathbf{p}_0) \odot \bar{\mathbf{f}}(\mathbf{p}|\mathbf{p}_0), \quad (123)$$

$$= \frac{K_0^2 \cos^2 \theta}{(2\pi)^2} \bar{\mathbf{R}}(\mathbf{p}|\mathbf{p}_0) \odot \bar{\mathbf{R}}(\mathbf{p}|\mathbf{p}_0). \quad (124)$$

Following Ishimaru *et al.*,<sup>31</sup> we define the Mueller matrix cross section per unit area  $\bar{\sigma} = (\sigma_{ij})$ ,

$$\bar{\sigma} \equiv \frac{4\pi}{A} \bar{\mathbf{M}}, \quad (125)$$

and, the bistatic Mueller matrix<sup>4</sup>  $\bar{\gamma} = (\gamma_{ij})$ :

$$\bar{\gamma} \equiv \frac{1}{A \cos \theta_0} \bar{\mathbf{M}}. \quad (126)$$

These matrices are generalizations of the classical coefficients. In fact, if we assume, for example, that the incident wave is vertically polarized, we have

$$\frac{1}{A \cos \theta_0} |E_V^s(\mathbf{p})|^2 = \frac{1}{\|\mathbf{r}\|^2} \gamma_{11}(\mathbf{p}|\mathbf{p}_0) |E_V^i(\mathbf{p})|^2, \quad (127)$$

$$\frac{1}{A \cos \theta_0} |E_H^s(\mathbf{p})|^2 = \frac{1}{\|\mathbf{r}\|^2} \gamma_{21}(\mathbf{p}|\mathbf{p}_0) |E_V^i(\mathbf{p})|^2. \quad (128)$$

Thus  $\gamma_{11}$  and  $\gamma_{21}$  are the classical bistatic coefficients  $\gamma_{VV}$  and  $\gamma_{HV}$ , respectively. We can also define the cross section

and the bistatic coefficients for an incident circular polarization. As an example, taking the incident wave to be right circularly polarized, we have

$$\mathbf{I}^i(\mathbf{p}_0) = \frac{1}{2}(1 \ 1 \ 0 \ -2)^t. \quad (129)$$

Now, if we put a right-hand side polarizer at the receiver,

$$\frac{1}{4} \begin{pmatrix} 1 & 1 & 0 & 1 \\ 1 & 1 & 0 & 1 \\ 0 & 0 & 0 & 0 \\ 2 & 2 & 0 & 2 \end{pmatrix}. \quad (130)$$

the right to right bistatic coefficient  $\gamma_{rr}$  is

$$\begin{aligned} \gamma_{rr} = & \frac{1}{4}(\gamma_{11} + \gamma_{12} + 2\gamma_{14} + \gamma_{21} + \gamma_{22} + 2\gamma_{24} + \gamma_{41} \\ & + \gamma_{42} + 2\gamma_{44}), \end{aligned} \quad (131)$$

where  $\gamma_{ij}$  are coefficients of the matrix  $\bar{\gamma} = (\gamma_{ij})$ .

In a similar way, we obtain the right to left bistatic coefficient

$$\begin{aligned} \gamma_{lr} = & \frac{1}{4}(\gamma_{11} + \gamma_{12} + 2\gamma_{14} + \gamma_{21} + \gamma_{22} + 2\gamma_{24} - \gamma_{41} \\ & - \gamma_{42} - 2\gamma_{44}). \end{aligned} \quad (132)$$

Up to now, we have made no hypothesis on the nature of the rough surface. Let us introduce the statistical characteristics of the function  $h(\mathbf{x})$ . We suppose that it is a stationary, isotropic Gaussian random process defined by the moments

$$\langle h(\mathbf{x}) \rangle = 0, \quad (133)$$

$$\langle h(\mathbf{x})h(\mathbf{x}') \rangle = W(\mathbf{x} - \mathbf{x}'), \quad (134)$$

where the angle brackets denote an average over the ensemble of realizations of the function  $h(\mathbf{x})$ . In this work we will use a Gaussian form for the surface-height correlation function  $W(\mathbf{x})$ ,

$$W(\mathbf{x}) = \sigma^2 \exp(-\mathbf{x}^2/l^2), \quad (135)$$

where  $\sigma$  is the rms height of the surface, and  $l$  is the transverse correlation length. In momentum space we have

$$\langle h(\mathbf{p}) \rangle = 0, \quad (136)$$

$$\langle h(\mathbf{p})h(\mathbf{p}') \rangle = (2\pi)^2 \delta(\mathbf{p} + \mathbf{p}') W(\mathbf{p}), \quad (137)$$

with

$$W(\mathbf{p}) \equiv \int d^2\mathbf{x} W(\mathbf{x}) \exp(-i\mathbf{p} \cdot \mathbf{x}) \quad (138)$$

$$= \pi \sigma^2 l^2 \exp(-\mathbf{p}^2 l^2 / 4). \quad (139)$$

We are now able to define the bistatic coherent matrix

$$\begin{aligned} \bar{\gamma}^{\text{coh}}(\mathbf{p}|\mathbf{p}_0) & \equiv \frac{1}{A \cos \theta_0} \langle \bar{\mathbf{f}}(\mathbf{p}|\mathbf{p}_0) \odot \bar{\mathbf{f}}(\mathbf{p}|\mathbf{p}_0) \rangle \\ & = \frac{K_0^2 \cos^2 \theta}{A (2\pi)^2 \cos \theta_0} \langle \bar{\mathbf{R}}(\mathbf{p}|\mathbf{p}_0) \odot \bar{\mathbf{R}}(\mathbf{p}|\mathbf{p}_0) \rangle, \end{aligned} \quad (140)$$

and the incoherent bistatic matrix

$$\begin{aligned} \bar{\gamma}^{\text{incoh}}(\mathbf{p}|\mathbf{p}_0) & \equiv \frac{1}{A \cos \theta_0} [\langle \bar{\mathbf{f}}(\mathbf{p}|\mathbf{p}_0) \odot \bar{\mathbf{f}}(\mathbf{p}|\mathbf{p}_0) \rangle \\ & \quad - \langle \bar{\mathbf{f}}(\mathbf{p}|\mathbf{p}_0) \rangle \odot \langle \bar{\mathbf{f}}(\mathbf{p}|\mathbf{p}_0) \rangle], \\ & = \frac{K_0^2 \cos^2 \theta}{A (2\pi)^2 \cos \theta_0} [\langle \bar{\mathbf{R}}(\mathbf{p}|\mathbf{p}_0) \odot \bar{\mathbf{R}}(\mathbf{p}|\mathbf{p}_0) \rangle \\ & \quad - \langle \bar{\mathbf{R}}(\mathbf{p}|\mathbf{p}_0) \rangle \odot \langle \bar{\mathbf{R}}(\mathbf{p}|\mathbf{p}_0) \rangle]. \end{aligned} \quad (141)$$

From Eq. (53), and the property of the Gaussian random process, we obtain

$$\bar{\gamma}^{\text{coh}}(\mathbf{p}|\mathbf{p}_0) = \frac{K_0^2 \cos^2 \theta}{\cos \theta_0} \delta(\mathbf{p} - \mathbf{p}_0) \bar{\mathbf{R}}^{\text{coh}}(\mathbf{p}_0) \odot \bar{\mathbf{R}}^{\text{coh}}(\mathbf{p}_0), \quad (142)$$

$$\begin{aligned} \bar{\mathbf{R}}^{\text{coh}}(\mathbf{p}_0) & \equiv \bar{\mathbf{X}}^{(0)}(\mathbf{p}_0) + K_0 \cos \theta_0 \int \frac{d^2\mathbf{p}}{(2\pi)^2} \\ & \quad \bar{\mathbf{X}}^{(2)}(\mathbf{p}_0|\mathbf{p}_1|\mathbf{p}_0) W(\mathbf{p}_1 - \mathbf{p}_0) + \dots, \end{aligned} \quad (143)$$

where  $\bar{\mathbf{R}}^{\text{coh}}(\mathbf{p}_0)$  is a diagonal matrix describing the reflection coefficients of the coherent waves. For the incoherent part we have

$$\begin{aligned} \bar{\gamma}^{\text{incoh}}(\mathbf{p}|\mathbf{p}_0) & = \frac{K_0^4 \cos^2 \theta \cos \theta_0}{(2\pi)^2} [\bar{\mathbf{I}}^{(1-1)}(\mathbf{p}|\mathbf{p}_0) + \bar{\mathbf{I}}^{(2-2)}(\mathbf{p}|\mathbf{p}_0) \\ & \quad + \bar{\mathbf{I}}^{(3-1)}(\mathbf{p}|\mathbf{p}_0)], \end{aligned} \quad (144)$$

where

$$\bar{\mathbf{I}}^{(1-1)}(\mathbf{p}|\mathbf{p}_0) \equiv W(\mathbf{p} - \mathbf{p}_0) \bar{\mathbf{X}}^{(1)}(\mathbf{p}|\mathbf{p}_0) \odot \bar{\mathbf{X}}^{(1)}(\mathbf{p}|\mathbf{p}_0), \quad (145)$$

$$\begin{aligned} \bar{\mathbf{I}}^{(2-2)}(\mathbf{p}|\mathbf{p}_0) & \equiv \int \frac{d^2\mathbf{p}_1}{(2\pi)^2} W(\mathbf{p} - \mathbf{p}_1) W(\mathbf{p}_1 - \mathbf{p}_0) \\ & \quad \bar{\mathbf{X}}^{(2)}(\mathbf{p}|\mathbf{p}_1|\mathbf{p}_0) \odot [\bar{\mathbf{X}}^{(2)}(\mathbf{p}|\mathbf{p}_1|\mathbf{p}_0) \\ & \quad + \bar{\mathbf{X}}^{(2)}(\mathbf{p}|\mathbf{p} + \mathbf{p}_0 - \mathbf{p}_1|\mathbf{p}_0)], \end{aligned} \quad (146)$$

$$\begin{aligned} \bar{\mathbf{I}}^{(3-1)}(\mathbf{p}|\mathbf{p}_0) & \equiv W(\mathbf{p} - \mathbf{p}_0) [\bar{\mathbf{X}}^{(1)}(\mathbf{p}|\mathbf{p}_0) \odot \bar{\mathbf{X}}^{(3)}(\mathbf{p}|\mathbf{p}_0) \\ & \quad + \bar{\mathbf{X}}^{(3)}(\mathbf{p}|\mathbf{p}_0) \odot \bar{\mathbf{X}}^{(1)}(\mathbf{p}|\mathbf{p}_0)], \end{aligned} \quad (147)$$

with

$$\begin{aligned} \bar{\mathbf{X}}^{(3)}(\mathbf{p}|\mathbf{p}_0) & \equiv \int \frac{d^2\mathbf{p}_1}{(2\pi)^2} \{ W(\mathbf{p}_1 - \mathbf{p}_0) \bar{\mathbf{X}}^{(3)}(\mathbf{p}|\mathbf{p}_0|\mathbf{p}_1|\mathbf{p}_0) \\ & \quad + W(\mathbf{p} - \mathbf{p}_1) [\bar{\mathbf{X}}^{(3)}(\mathbf{p}|\mathbf{p}_1|\mathbf{p}_0 - \mathbf{p} + \mathbf{p}_1|\mathbf{p}_0) \\ & \quad + \bar{\mathbf{X}}^{(3)}(\mathbf{p}|\mathbf{p}_1|\mathbf{p}|\mathbf{p}_0)] \}. \end{aligned} \quad (148)$$

## VI. APPLICATIONS

In the previous sections we have developed a method to compute the scattering matrices for a rough surface between

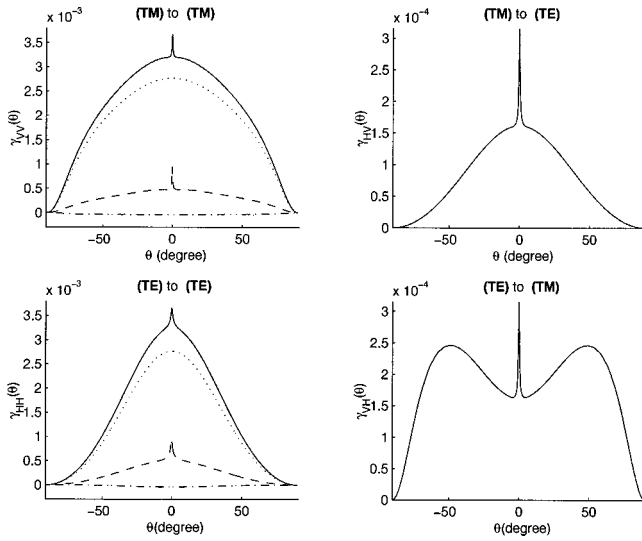


FIG. 8. The bistatic coefficients for horizontal (TE) and vertical (TM) polarized incident light of wavelength  $\lambda = 457.9$  nm ( $\theta_0 = 0^\circ$  and  $\phi = \phi_0 = 0^\circ$ ), on a two-dimensional randomly rough silver surface, characterized by the parameters  $\sigma = 5$  nm,  $l = 100$  nm and  $\epsilon_1 = -7.5 + i0.24$ . For each figure are plotted the total incoherent scattering  $\bar{\gamma}^{\text{incoh}}$  (solid curve), the first order given by  $\bar{\mathbf{I}}^{(1-1)}$  (dotted line), the second order by  $\bar{\mathbf{I}}^{(2-2)}$  (dashed line), and the third order by  $\bar{\mathbf{I}}^{(3-1)}$  (dash-dotted line).

two media, and for a thin film which includes one rough surface. In this section, we will numerically evaluate the incoherent bistatic coefficients given by Eqs. (144)–(147) for different values of the parameters which characterize the configurations. In all numerical simulations the media 0 will be the vacuum ( $\epsilon_0 = 1$ ).

### A. A rough surface separating to different media

We consider that a polarized light of wavelength  $\lambda = 457.9$  nm is normally incident ( $\theta_0 = 0^\circ$ ,  $\phi_0 = 0^\circ$ ) on a two-dimensional rough silver surface (see Fig. 3) characterized by the roughness parameters  $\sigma = 5$  nm,  $l = 100$  nm, and  $\epsilon = -7.5 + i0.24$ . As a matter of comparison we have chosen the same parameters used for the scattering by a one-dimensional rough surface.<sup>21</sup> The perturbative development is given by Eqs. (61)–(68). In Fig. 8, we present the results for an incident wave linearly polarized, the scattered field being observed in the incident plane ( $\phi = 0^\circ$ ). The single-scattering contribution associated with the term  $\bar{\mathbf{I}}^{(1-1)}$  is plotted as a dotted line, the double-scattering contribution  $\bar{\mathbf{I}}^{(2-2)}$  as a dashed line, the scattering term  $\bar{\mathbf{I}}^{(3-1)}$  as a dash-dotted line, and the sum of all these terms  $\bar{\gamma}^{\text{incoh}}$  by the solid curve.

We observed an enhancement of the backscattering which corresponds to the physical process in which the incident light excites a surface electromagnetic wave. In fact, the surface polariton propagates along the rough surface, and is then scattered into a volume wave due to the roughness. At

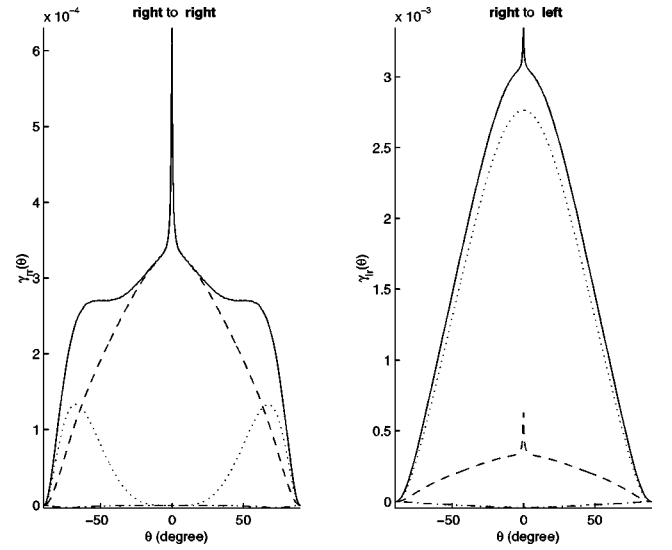


FIG. 9. The same configuration as in Fig. 8, but with a right incident circularly polarized wave, and right to right (or left to left) and right to left (or left to right) observed polarizations.

the same time, a reverse partner exists with a path travelling in the opposite direction. These two paths can interfere constructively near the backscattering direction to produce a peak.<sup>17–19</sup> However, in one dimension,<sup>21</sup> this peak can only be observed for a TM-polarized incident wave because a surface polariton only exists for this polarization. In two dimensions, the surface wave also exists for a TE polarization, but in fact a depolarization occurs so that a TE incident wave can excite a TM surface wave, and this surface wave can be scattered into volume wave with both polarizations as can be seen in Fig. 8. Now, when the incident wave is circularly polarized, we see, in Fig. 9, that enhanced backscattering takes also place. We have not displayed the left to left and left to right polarizations because the media are not optically active; as a consequence, the results are the same whether the incident wave is right or left polarized.

In expression (144), the peak is produced by the term  $\bar{\mathbf{I}}^{(2-2)}$ . We see that the term  $\bar{\mathbf{P}}(\mathbf{u}|\mathbf{p}_1) \cdot \bar{\mathbf{Q}}^+(\mathbf{p}_1|\mathbf{p}_0)$  in  $\bar{\mathbf{X}}_{s\epsilon_0, \epsilon_1}^{(2)}(\mathbf{p}|\mathbf{p}_1|\mathbf{p}_0)$  contains a factor of the form [see Eq. (58)]

$$[D_{10VV}^+(\mathbf{p}_1)]^{-1} = \frac{1}{\epsilon_1 \alpha_0(\mathbf{p}_1) + \epsilon_0 \alpha_1(\mathbf{p}_1)}, \quad (149)$$

which is close to zero except when  $\mathbf{p}_1$  is near the resonance mode  $\mathbf{p}_r$  of the polariton, which is given by the roots  $D_{10VV}^+(\mathbf{p}_r) = 0$ . When we observe a field scattered far away from the backscattering direction ( $\mathbf{p} + \mathbf{p}_0 \neq 0$ ), the terms  $\bar{\mathbf{X}}_{s\epsilon_0, \epsilon_1}^{(2)}(\mathbf{p}|\mathbf{p}_1|\mathbf{p}_0)$  and  $\bar{\mathbf{X}}_{s\epsilon_0, \epsilon_1}^{(2)}(\mathbf{p}|\mathbf{p} + \mathbf{p}_0 - \mathbf{p}_1|\mathbf{p}_0)$ , containing  $D_{10VV}^+$ , are nonzero when  $\mathbf{p}_1 \approx \mathbf{p}_r$ , and  $\mathbf{p} + \mathbf{p}_0 - \mathbf{p}_1 \approx \mathbf{p}_r$ , respectively. Since these domains are disjointed, the product  $\odot$  of these two terms is approximately zero. Conversely, when we are near the backscattering direction ( $\mathbf{p} + \mathbf{p}_0 \approx 0$ ), the terms inside the brackets are almost equal and produce an

enhancement factor. This enhancement factor is not equal to 2 because the matrices  $\bar{\mathbf{Q}}^+(\mathbf{p}|\mathbf{p}_0)$  and  $\bar{\mathbf{Q}}^-(\mathbf{p}|\mathbf{p}_0)$  in  $\bar{\mathbf{X}}_{s\epsilon_0, \epsilon_1}^{(2)}$  do not contain the term  $[D_{10VV}^+(\mathbf{p}_1)]^{-1}$ , so they produce a significant contribution whatever the scattering angle is. In order to isolate the terms producing an enhanced backscattering more precisely, a better approach is to work with the formalism of Ref. 16 derived from quantum-mechanical scattering theory; such an approach was used, for instance, in Refs. 17 and 23. If the decomposition of each step of the multiple-scattering process is clearly put in evidence, however, it offers the disadvantage of producing a heavier perturbative development, as can be seen when comparing Eqs. (53) and (66)–(68) with Eqs. (15)–(19) and (A-1) of Ref. 22.

### B. A film with a rough surface on the upper side

We consider a dielectric film (see Fig. 7), of mean thickness  $H=500$  nm and dielectric constant  $\epsilon_1=2.6896+0.0075i$ , deposited on a planar perfectly conducting substrate ( $\epsilon_2=i\infty$ ), and illuminated by a linearly polarized light of normally incident wavelength  $\lambda=632.8$  nm ( $\phi_0=0^\circ, \theta_0=0^\circ$ ). The two-dimensional upper rough surface is characterized by the parameters  $\sigma=15$  nm and  $l=100$  nm. The scattering diagrams are shown in Fig. 10, with the same curve labeling as before. The perturbative development is given by Eqs. (105), (107), (110), and (116). Since we have chosen an infinite conducting plane ( $\epsilon_2=i\infty$ ), the coefficients  $F^\pm$  [Eq. (114)] have the following forms:

$$F_V^\pm(\mathbf{p}_0) = \frac{1 \pm \exp[2i\alpha_0(\mathbf{p}_0)H]}{[\epsilon_1\alpha_0(\mathbf{p}_0) + \epsilon_0\alpha_1(\mathbf{p}_0)] + [\epsilon_1\alpha_0(\mathbf{p}_0) - \epsilon_0\alpha_1(\mathbf{p}_0)]\exp[2i\alpha_0(\mathbf{p}_0)H]}, \quad (150)$$

$$F_H^\pm(\mathbf{p}_0) = \frac{1 \mp \exp[2i\alpha_0(p_0)H]}{[\alpha_0(\mathbf{p}_0) + \alpha_1(\mathbf{p}_0)] + [\alpha_0(\mathbf{p}_0) - \alpha_1(\mathbf{p}_0)]\exp[2i\alpha_0(\mathbf{p}_0)H]}, \quad (151)$$

The parameters are the same as those used in Ref. 23 for a one-dimensional dielectric film where a TE-polarized wave is incident. The thickness was chosen in such a way that the slab supports only two guided wave modes  $p_{\text{TE}}^1=1.5466K_0$  and  $p_{\text{TE}}^2=1.2423K_0$  for the TE polarization. These modes are resonance modes; they verify  $[F_H^\pm]^{-1}(p_{\text{TE}}^{1,2})=0$ . For the TM case, we have three modes given by the roots  $[F_V^\pm]^{-1}(p_{\text{TM}})=0$ , which are  $p_{\text{TM}}^1=1.6126K_0$ ,  $p_{\text{TM}}^2=1.3823K_0$ , and  $p_{\text{TM}}^3=1.0030K_0$ . As described in Refs. 11, 23, and 32, these guided modes can produce a classically enhanced backscattering with satellite peaks symmetrically positioned. The satellite peaks angles are given by the equation

$$\sin \theta_\pm^{nm} = -\sin \theta_0 \pm \frac{1}{K_0}[p^n - p^m], \quad (152)$$

where  $p^n$  and  $p^m$  describe one of the guided modes. When  $n=m$ , we recover the classical enhanced backscattering. We can give an explanation for this formula as in the previous case. In expression (106), the term producing the peaks comes from

$$-2\bar{\mathbf{P}}(\mathbf{u}|\mathbf{p}_1) \cdot \bar{\mathbf{Q}}^+(\mathbf{p}_1|\mathbf{p}_0), \quad (153)$$

where  $\bar{\mathbf{Q}}^+(\mathbf{p}_1|\mathbf{p}_0)$  contains the factors  $F^\pm(\mathbf{p}_1)$  having resonances for the slab guided mode. The product

$$\bar{\mathbf{X}}_d^{(2)}(\mathbf{p}|\mathbf{p}_1|\mathbf{p}_0) \odot \bar{\mathbf{X}}_d^{(2)}(\mathbf{p}|\mathbf{p}+\mathbf{p}_0-\mathbf{p}_1|\mathbf{p}_0) \quad (154)$$

in Eq. (146) has a significant contribution only when  $\mathbf{p}_1$  and  $\mathbf{p}+\mathbf{p}_0-\mathbf{p}_1$  are near resonance modes. As there are several resonances, we can have  $\mathbf{p}_1 \approx \mathbf{p}^n$  and  $\mathbf{p}+\mathbf{p}_0-\mathbf{p}_1 \approx \mathbf{p}^m$ , with  $n \neq m$ , where  $\mathbf{p}^n$  and  $\mathbf{p}^m$  are resonance vectors. If  $\mathbf{p}^n$

$= \pm p^n \hat{\mathbf{e}}_x$  and  $\mathbf{p}^m = \mp p^m \hat{\mathbf{e}}_x$  (guided modes propagating along the incident plane but with opposite directions), we have  $(\mathbf{p} + \mathbf{p}_0) \cdot \hat{\mathbf{e}}_x \approx \pm(p^n - p^m)$  which is another way of writing Eq. (152). For the TE polarization, since we have only two guided waves, the satellite peaks can only exist at the angles  $\theta_\pm^{12}(\text{TE}) = \pm 17.7^\circ$ . Now, for the TM polarization we have three possibilities:  $\theta_\pm^{12}(\text{TM}) = \pm 13.3^\circ$ ,  $\theta_\pm^{13}(\text{TM}) = \pm 37.6^\circ$ , and  $\theta_\pm^{23}(\text{TM}) = \pm 22.3^\circ$ . The satellite peaks are produced by the term  $\bar{\mathbf{I}}^{(2-2)}$ , and in the case of TM polarization we do not obtain any significant contribution to satellite peaks. However, for the TE to TE scattering shown in Fig. 11, we find satellite peaks at the angle  $\theta_\pm^{12}(\text{TE}) = \pm 17.7^\circ$  positioned along a dotted line. Now, by doubling the slab thickness (see Fig. 12), the satellite peaks disappear for the entry polarization, but we see a phenomenon called Selényi fringes.<sup>32-34</sup> For a slightly random rough surface, the slab produces fringes similar to those obtained with a Fabry-Perrot interferometer illuminated by an extended source. The roughness modulates amplitude fringes, but their localization remains the same as for the interferometer. We also note that the enhanced backscattering decreases with the slab thickness. We can conclude, as in the case of one-dimensional rough surface, that the satellite peaks appear only when the waveguide supports few modes for the TE polarizations. These results differ from those obtained in Ref. 32 where no satellite peak appears in their two-dimensional slab. We have checked that with these parameters values we also find no peak, and we agree with the results given by the contributions of the first- and second-order terms. However, the third order term gives a contribution larger than the first-order one, and such a result casts some doubt on the validity of the SPM method in that case.

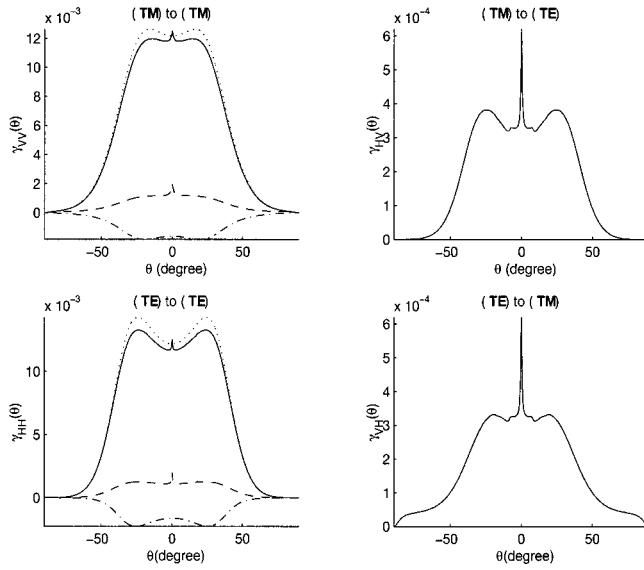


FIG. 10. The bistatic coefficients for horizontal (TE) and vertical (TM) polarized incident light of wavelength  $\lambda = 632.8$  nm, on a slab with an upper two-dimensional randomly rough surface, characterized by the parameters  $\sigma = 15$  nm,  $l = 100$  nm,  $\epsilon_1 = 2.6896 + i0.0075$ , and thickness  $H = 500$  nm, deposited on an infinite conducting plane ( $\epsilon_2 = -\infty$ ). The scattered field is observed in the incident plane. For each figure are plotted the total incoherent scattering  $\bar{\gamma}^{\text{incoh}}$  (solid curve), the first order given by  $\bar{\Gamma}^{(1-1)}$  (dotted line), the second order by  $\bar{\Gamma}^{(2-2)}$  (dashed line), and the third order by  $\bar{\Gamma}^{(3-1)}$  (dash-dotted line).

However, for the choice of parameters presented here, no satellite peak has been observed even when the thickness of the slab is chosen in such a way that only two guided modes exist for the TM polarization (a result not presented here). This is in agreement with the results of Ref. 35 for a one-

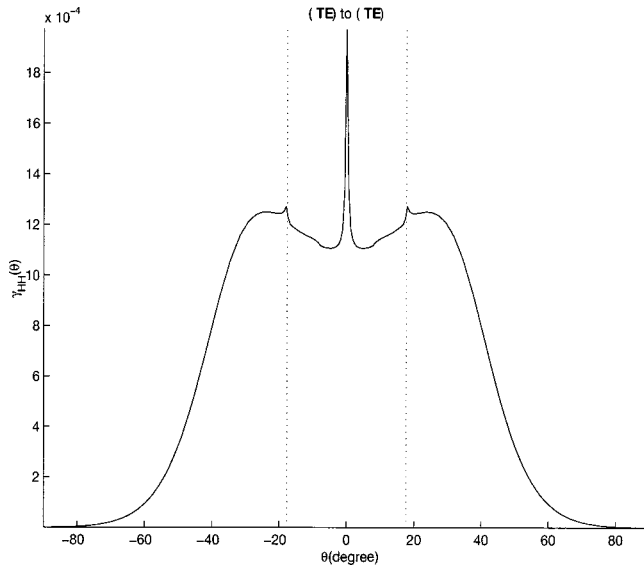


FIG. 11. Details of the second-order (TE to TE) contribution to the scattering shown in Fig. 10. We see two satellite peaks at the angle  $\theta_{\pm}^{12}(\text{TE}) = \pm 17.7^\circ$ . The dotted lines mark the peak angle position.

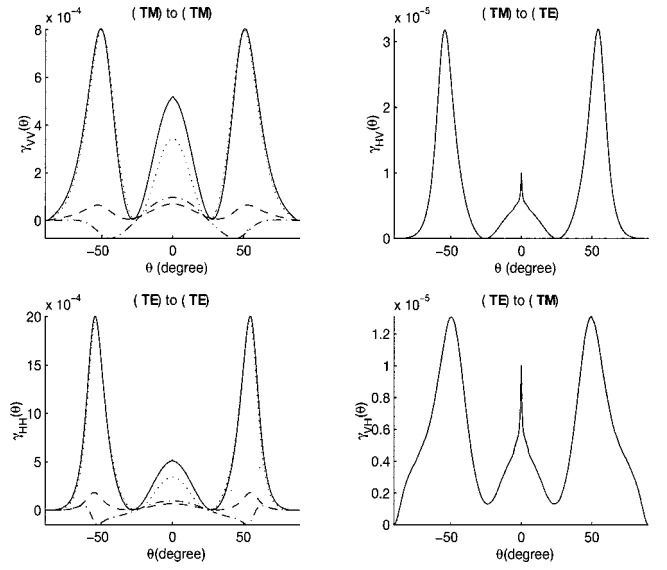


FIG. 12. Effect of the slab thickness  $H = 1000$  nm on the configuration shown in Fig. 10.

dimensional surface, where it is noted that the excitation of TM modes are more difficult to excite than the TE modes. In order to enhance this effect the authors of Ref. 35 chose a higher permittivity for the media 1.  $\epsilon_1 = 5.6644 + i0.005$ . In this case satellite peaks were observed for a slab which supports three guided modes. We have also done numerical calculations with these parameters; however, we did not observe satellite peaks. Thus the transition from one- to two-dimensional rough surfaces lowers the efficiency of the excitation of TM modes. Next, instead of doubling the slab thickness, we have changed the infinite conducting plane by a silver plane ( $\epsilon_2 = -18.3 + 0.55i$ ). We see in Fig. 13 that the enhancement of backscattering is also decreased, and that there is no more satellite peak corresponding to TE to TE scattering. This fact has to be compared with the next configuration, where the rough surface is now between media 1 and 2; see Fig. 4.

### C. A film with a rough surface on the bottom side

The permittivities are the same as in the previous configuration, except that the case  $\epsilon_2 = i\infty$  cannot be treated with the SPM because the second and third orders diverge. The rms height  $\sigma$  now has values  $\sigma = 5$  nm and  $l = 100$  nm. We have not chosen  $\sigma = 15$  nm because numerically we note that the first-order term  $\bar{\Gamma}^{(1-1)}$  was not greater than the second order  $\bar{\Gamma}^{(2-2)}$ , which means that we are near the limit of validity of the SPM. The perturbative development is given by Eqs. (97)–(99), and the guided modes are the roots of  $[X_{Vd}^{(0)}(p_{\text{TM}})]^{-1}$  for TM polarization, and of  $[X_{Hd}^{(0)}(p_{\text{TE}})]^{-1}$  for TE polarization. We obtain two modes in the TE case, whose values are  $p_{\text{TE}}^1 = 1.5534K_0$  and  $p_{\text{TE}}^2 = 1.2727K_0$ ; the corresponding satellite peaks angles are  $\theta_{\pm}^{12}(\text{TE}) = \pm 16.3^\circ$ . For the TM case, we have three guided modes with  $p_{\text{TM}}^1 = 1.7752K_0$ ,  $p_{\text{TM}}^2 = 1.4577K_0$ , and  $p_{\text{TM}}^3 = 1.034K_0$ ; they correspond to six possible satellite peaks

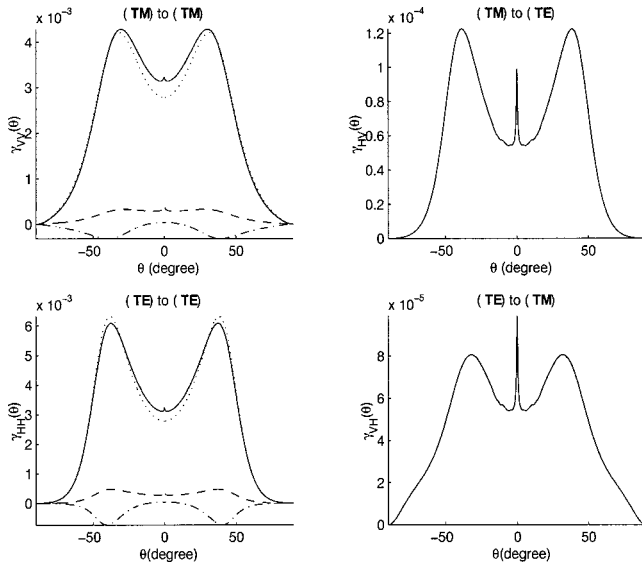


FIG. 13. The same parameters as in Fig. 10, but with a silver plane characterized by  $\epsilon_2 = -18.3 + 0.55i$ .

angles given by  $\theta_{\pm}^{12}(\text{TM}) = \pm 18.51^\circ$ ,  $\theta_{\pm}^{13}(\text{TM}) = \pm 47.8^\circ$ , and  $\theta_{\pm}^{23}(\text{TM}) = \pm 25^\circ$ . We see the apparition of satellite peaks only for the TM to TM scattering process, as shown in Fig. 14. This result differs from the previous case because, on the one hand, the rough surface not being a perfect conductor, we still obtain satellite peaks; on the other hand, these satellite peaks now appear for the TM to TM polariza-

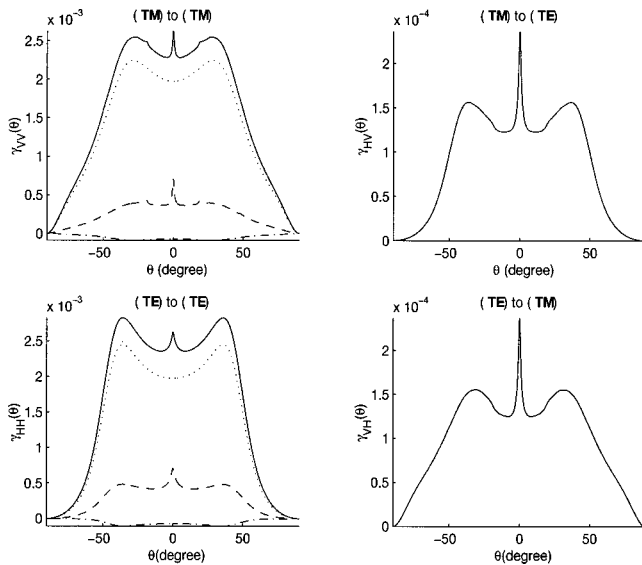


FIG. 14. The bistatic coefficients for horizontal (TE) and vertical (TM) polarized light of wavelength  $\lambda = 632.8$  nm, incident on a film of permittivity  $\epsilon_1 = 2.6896 + i0.0075$ , deposited on a two-dimensional randomly rough surface, characterized by the parameters  $\sigma = 5$  nm,  $l = 100$  nm,  $\epsilon_2 = -18.3 + 0.55i$ , and thickness  $H = 500$  nm. The scattered field is observed in the incident plane. For each figure are plotted the total incoherent scattering  $\bar{\gamma}^{\text{incoh}}$  (solid curve), the first order given by  $\bar{\mathbf{I}}^{(1-1)}$  (dotted line), the second order by  $\bar{\mathbf{I}}^{(2-2)}$  (dashed line), and the third order by  $\bar{\mathbf{I}}^{(3-1)}$  (dash-dotted line).

tion instead of the TE to TE polarization. This is a surprising result, because the TM polarization, which has one more mode than the TE one, should decrease the amplitude of the satellite peaks for this polarization, as was the case with an upper rough boundary. Moreover, we see in Fig. 15 that the three satellite peaks can be clearly separated. This can be explained from the fact that there are two phenomena which occur in this case. The first is the same as in the previous case, where the wave can excite guided modes through the roughness, which produces an enhancement of backscattering and the satellite peaks. These effects come from the term

$$\alpha_1(\mathbf{p}_1) \bar{\mathbf{X}}_{s\epsilon_1, \epsilon_2}^{H(1)}(\mathbf{p}|\mathbf{p}_1) \cdot \bar{\mathbf{U}}^{(0)}(\mathbf{p}_1) \cdot \bar{\mathbf{V}}^{10}(\mathbf{p}_1) \cdot \bar{\mathbf{X}}_{s\epsilon_1, \epsilon_2}^{H(1)}(\mathbf{p}_1|\mathbf{p}_0) \quad (155)$$

in Eq. (98), where  $\bar{\mathbf{U}}^{(0)}(\mathbf{p}_1)$  have resonances for the different modes of the guided wave. However, there is also a second phenomenon which was described in our first example, where the rough surface can excite a plasmon mode. This appears from Eq. (98), with the term

$$\bar{\mathbf{X}}_{s\epsilon_1, \epsilon_2}^{H(2)}(\mathbf{p}|\mathbf{p}_1|\mathbf{p}_0), \quad (156)$$

and subsequently in Eqs. (144) and (146). The localization of this mode  $\mathbf{p}_r$  is given by

$$[D_{21VV}^+(\mathbf{p}_r)]^{-1} = \frac{1}{\epsilon_2 \alpha_1(\mathbf{p}_r) + \epsilon_1 \alpha_2(\mathbf{p}_r)}. \quad (157)$$

In our case this gives  $\|\mathbf{p}_r\| = 1.7755K_0$ , which is very close to the value  $p_{\text{TM}}^1 = 1.7752K_0$ . So, in Eq. (146) the product  $\odot$  of Eq. (155) by Eq. (156) can produce peaks where  $\mathbf{p}_1 = \pm \|\mathbf{p}_r\| \hat{e}_x \approx \pm p_{\text{TM}}^1 \hat{e}_x$  and  $(\mathbf{p}_0 + \mathbf{p}) \cdot \hat{e}_x = \pm (p_{\text{TM}}^1 - p_{\text{TM}}^n)$ , with  $n = 1, 2$ , and  $3$ . We have effectively verified numerically that the product of this two term can considerably enhance the different peaks, in particular the first satellite peaks  $\theta_{\pm}^{12}$  (when  $n = 2$ ). Now, by doubling the slab thickness, we see

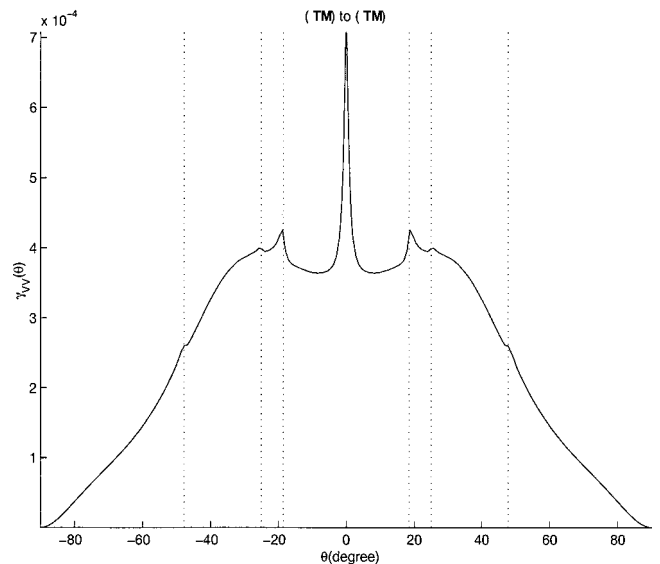


FIG. 15. Details of the second-order (TM to TM) contribution to the scattering shown in Fig. 14. Dotted lines mark the peak angle position.

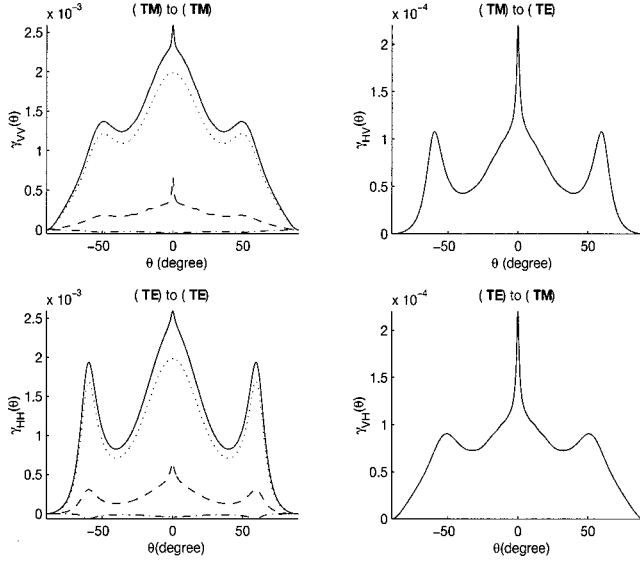


FIG. 16. Effect of the slab thickness  $H=1000$  nm on the configuration shown in Fig. 14.

from Fig. 16 that the satellite peaks have disappeared due to the profusion of guided modes which can be excited.

## VII. CONCLUSIONS

We have obtained four generalized reduced Rayleigh equations which are exact integral equations, and where one of the four unknown fields coming on the rough surface has been eliminated. These equations offer a systematic method to compute the small perturbation development without lengthy calculations. Moreover, the scattering matrices are only two dimensional. All the theoretical calculations have been done up to order 3 in the height elevation, which allowed us to obtain all the fourth-order cross-section terms. We have calculated the perturbative development for three

different structures composed of a rough surface separating to semi-infinite media, and a dielectric film where one of the two boundaries is a rough surface. For the first structure, the perturbative expression was already calculated at the third order, but our derivation offers the advantage that it can be formulated in a compact manner, making numerical computations easier. For the slab configuration we present new results, to our knowledge. It should be noted that for the case of a rough surface in the upper position, a generalized derivation of the reduced Rayleigh equations becomes mandatory. The numerical results show an enhancement of the backscattering for co-polarization and cross-polarization in all these cases. In the slab case, for some configurations and definite polarizations, we have detected satellite peaks which result from the interference of different waveguide modes. This general formulation can be extended to a configuration including two rough surfaces, and some results will be presented in a next subsequent paper.<sup>36</sup>

## ACKNOWLEDGMENT

A. S. thanks ANRT for financial support during the preparation of his thesis (Contract No. CIFRE-238-98).

## APPENDIX A: INTEGRATION BY PARTS

We need to calculate the following integral:

$$\int d^2\mathbf{x} \exp[-i(\mathbf{k}_u^{1b} - \mathbf{k}_p^{1a}) \cdot \mathbf{r}_x] \nabla h(\mathbf{x}). \quad (\text{A1})$$

Since  $\nabla h(x,y)$  is zero for  $|x| \geq L/2$  or  $|y| \geq L/2$ , we can fix the integration limits. We choose the boundary limits  $x_l$  in  $x$  such that  $|x_l| > L/2$ , and  $(\mathbf{u} - \mathbf{p})_{x_l} = 2\pi m_x$ , with  $m_x \in \mathbb{Z}$ . Similarly, we choose the boundary  $y_l$  in  $y$  such that  $|y_l| > L/2$  and  $(\mathbf{u} - \mathbf{p})_{y_l} = 2\pi m_y$ , with  $m_y \in \mathbb{Z}$ . Thus the integral (A1) is

$$\begin{aligned} & \int_{-x_l}^{x_l} \int_{-y_l}^{y_l} dx dy \exp[-i(\mathbf{u} - \mathbf{p}) \cdot \mathbf{x}] \nabla h(\mathbf{x}) \exp\{-i[b\alpha_1(\mathbf{u}) - a\alpha_1(\mathbf{p})]h(\mathbf{x})\} \\ &= \hat{\mathbf{e}}_x \int_{-y_l}^{y_l} dy \left[ \frac{\exp\{-i(\mathbf{u} - \mathbf{p}) \cdot \mathbf{x} - i[b\alpha_1(\mathbf{u}) - a\alpha_1(\mathbf{p})]h(\mathbf{x})\}}{-i[b\alpha_1(\mathbf{u}) - a\alpha_1(\mathbf{p})]} \right]_{x=-x_l}^{x=+x_l} \\ &+ \hat{\mathbf{e}}_y \int_{-x_l}^{x_l} dx \left[ \frac{\exp\{-i(\mathbf{u} - \mathbf{p}) \cdot \mathbf{x} - i[b\alpha_1(\mathbf{u}) - a\alpha_1(\mathbf{p})]h(\mathbf{x})\}}{-i[b\alpha_1(\mathbf{u}) - a\alpha_1(\mathbf{p})]} \right]_{y=-y_l}^{y=+y_l} \\ &- \int_{-x_l}^{x_l} \int_{-y_l}^{y_l} \frac{-i(\mathbf{u} - \mathbf{p})}{-i[b\alpha_1(\mathbf{u}) - a\alpha_1(\mathbf{p})]} \exp\{-i(\mathbf{u} - \mathbf{p}) \cdot \mathbf{x} - i[b\alpha_1(\mathbf{u}) - a\alpha_1(\mathbf{p})]h(\mathbf{x})\} \end{aligned} \quad (\text{A2})$$

$$= - \int d^2\mathbf{x} \frac{(\mathbf{u} - \mathbf{p})}{[b\alpha_1(\mathbf{u}) - a\alpha_1(\mathbf{p})]} \exp[-i(\mathbf{k}_u^{1b} - \mathbf{k}_p^{1a}) \cdot \mathbf{r}_x]. \quad (\text{A3})$$

The term in the square bracket cancelled due to the choice made for  $x_l$  and  $y_l$ . From the previous calculations, we can now replace  $\nabla h(\mathbf{x})$  by

$$\nabla h(\mathbf{x}) \leftrightarrow - \frac{(\mathbf{u} - \mathbf{p})}{[b\alpha_1(\mathbf{u}) - a\alpha_1(\mathbf{p})]}. \quad (\text{A4})$$

### APPENDIX B: PERTURBATIVE DEVELOPMENT AND RECIPROCITY CONDITION

As noted by Voronovich,<sup>8</sup> the scattering operator  $\bar{\mathbf{R}}$  has a very simple law of transformation when we shift the boundary in the horizontal direction by a vector  $\mathbf{d}$ :

$$\bar{\mathbf{R}}_{\mathbf{x} \rightarrow h(\mathbf{x} - \mathbf{d})}(\mathbf{p}|\mathbf{p}_0) = \exp[-i(\mathbf{p} - \mathbf{p}_0) \cdot \mathbf{d}] \bar{\mathbf{R}}_{\mathbf{x} \rightarrow h(\mathbf{x})}(\mathbf{p}|\mathbf{p}_0), \quad (\text{B1})$$

or when we translate the surface by a vertical shift  $H\hat{\mathbf{e}}_z$ :

$$\bar{\mathbf{R}}_{h+H}(\mathbf{p}|\mathbf{p}_0) = \exp\{-i[\alpha_0\mathbf{p} + \alpha_0(\mathbf{p}_0)]H\} \bar{\mathbf{R}}_h(\mathbf{p}|\mathbf{p}_0). \quad (\text{B2})$$

Now, using Eq. (B1), we can deduce some properties on the perturbative development of the scattering operator. The generalization of the Taylor expansion for a function depending on a real variable to an expansion depending on a function (which is in fact a functional) can be expressed in the form

$$\bar{\mathbf{R}}(\mathbf{p}|\mathbf{p}_0) = \bar{\mathbf{R}}^{(0)}(\mathbf{p}|\mathbf{p}_0) + \bar{\mathbf{R}}^{(1)}(\mathbf{p}|\mathbf{p}_0) + \bar{\mathbf{R}}^{(2)}(\mathbf{p}|\mathbf{p}_0) + \bar{\mathbf{R}}^{(3)}(\mathbf{p}|\mathbf{p}_0) + \dots, \quad (\text{B3})$$

where

$$\bar{\mathbf{R}}^{(1)}(\mathbf{p}|\mathbf{p}_0) = \int \frac{d^2\mathbf{p}_1}{(2\pi)^2} \bar{\mathbf{R}}^{(1)}(\mathbf{p}|\mathbf{p}_1|\mathbf{p}_0) h(\mathbf{p}_1), \quad (\text{B4})$$

$$\bar{\mathbf{R}}^{(2)}(\mathbf{p}|\mathbf{p}_0) = \int \int \frac{d^2\mathbf{p}_1}{(2\pi)^2} \frac{d^2\mathbf{p}_2}{(2\pi)^2} \bar{\mathbf{R}}^{(2)}(\mathbf{p}|\mathbf{p}_1|\mathbf{p}_2|\mathbf{p}_0) h(\mathbf{p}_1) h(\mathbf{p}_2), \quad (\text{B5})$$

$$\bar{\mathbf{R}}^{(3)}(\mathbf{p}|\mathbf{p}_0) = \int \int \int \frac{d^2\mathbf{p}_1}{(2\pi)^2} \frac{d^2\mathbf{p}_2}{(2\pi)^2} \frac{d^2\mathbf{p}_3}{(2\pi)^2} \bar{\mathbf{R}}^{(3)}(\mathbf{p}|\mathbf{p}_1|\mathbf{p}_2|\mathbf{p}_3|\mathbf{p}_0) h(\mathbf{p}_1) h(\mathbf{p}_2) h(\mathbf{p}_3). \quad (\text{B6})$$

⋮

Applying this perturbative development on each side of Eq. (B1), and taking their functional derivative (see Ref. 7) defined by

$$\frac{\delta^{(n)}}{\delta h(\mathbf{q}_1) \dots \delta h(\mathbf{q}_n)}, \quad (\text{B7})$$

we obtain for all  $n \geq 0$ , in the limit  $h=0$ ,

$$\bar{\mathbf{R}}^{(n)}(\mathbf{p}|\mathbf{q}_1|\dots|\mathbf{q}_n|\mathbf{p}_0) = \exp[-i(\mathbf{p} - \mathbf{q}_1 \dots - \mathbf{q}_n - \mathbf{p}_0) \cdot \mathbf{d}] \times \bar{\mathbf{R}}^{(n)}(\mathbf{p}|\mathbf{q}_1|\dots|\mathbf{q}_n|\mathbf{p}_0). \quad (\text{B8})$$

We find that

$$\bar{\mathbf{R}}^{(n)}(\mathbf{p}|\mathbf{q}_1|\dots|\mathbf{q}_n|\mathbf{p}_0) \propto \delta(\mathbf{p} - \mathbf{q}_1 \dots - \mathbf{q}_n - \mathbf{p}_0) \quad (\text{B9})$$

so we can define  $\bar{\mathbf{X}}$  matrices by the relations

$$\bar{\mathbf{R}}^{(0)}(\mathbf{p}|\mathbf{p}_0) = (2\pi)^2 \delta(\mathbf{p} - \mathbf{p}_0) \bar{\mathbf{X}}^{(0)}(\mathbf{p}_0), \quad (\text{B10})$$

$$\bar{\mathbf{R}}^{(1)}(\mathbf{p}|\mathbf{p}_0) = \alpha_0(\mathbf{p}_0) \bar{\mathbf{X}}^{(1)}(\mathbf{p}|\mathbf{p}_0) h(\mathbf{p} - \mathbf{p}_0), \quad (\text{B11})$$

$$\bar{\mathbf{R}}^{(2)}(\mathbf{p}|\mathbf{p}_0) = \alpha_0(\mathbf{p}_0) \int \frac{d^2\mathbf{p}_1}{(2\pi)^2} \bar{\mathbf{R}}^{(2)}(\mathbf{p}|\mathbf{p}_1|\mathbf{p}_0) h(\mathbf{p} - \mathbf{p}_1) h(\mathbf{p}_1 - \mathbf{p}_0), \quad (\text{B12})$$

$$\bar{\mathbf{R}}^{(3)}(\mathbf{p}|\mathbf{p}_0) = \alpha_0(\mathbf{p}_0) \int \int \frac{d^2\mathbf{p}_1}{(2\pi)^2} \frac{d^2\mathbf{p}_2}{(2\pi)^2} \bar{\mathbf{R}}^{(3)}(\mathbf{p}|\mathbf{p}_1|\mathbf{p}_2|\mathbf{p}_0) h(\mathbf{p} - \mathbf{p}_1) h(\mathbf{p}_1 - \mathbf{p}_2) h(\mathbf{p}_2 - \mathbf{p}_0), \quad (\text{B13})$$

⋮

where  $\alpha_0(\mathbf{p}_0)$  is introduced for a matter of convenience.

Let us now make some remarks about the reciprocity condition. If we define the antitranspose operation by:

$$\begin{pmatrix} a & b \\ c & d \end{pmatrix}^{aT} = \begin{pmatrix} a & -c \\ -b & d \end{pmatrix}, \quad (\text{B14})$$

the reciprocity condition for an incident and a scattered waves in the medium 0 reads<sup>8</sup>

$$\frac{\bar{\mathbf{R}}^{aT}(\mathbf{p}|\mathbf{p}_0)}{\alpha_0(\mathbf{p}_0)} = \frac{\bar{\mathbf{R}}(-\mathbf{p}_0|-\mathbf{p})}{\alpha_0(\mathbf{p})}. \quad (\text{B15})$$

Making use of the previous functional derivative, we would like to prove that each order of the perturbative development must satisfies this condition. It is easy to show that

$$[\bar{\mathbf{X}}^{(1)}(\mathbf{p}|\mathbf{p}_0)]^{aT} = \bar{\mathbf{X}}^{(1)}(-\mathbf{p}_0|-\mathbf{p}), \quad (\text{B16})$$

thus  $\bar{\mathbf{X}}^{(1)}$  is reciprocal, but the same conclusion cannot be extended to  $\bar{\mathbf{X}}^{(n)}$  when  $n \geq 2$ . For example, in the case  $n=2$ , using Eq. (B15), we can only deduce that

$$\begin{aligned} & \int \frac{d^2\mathbf{p}_1}{(2\pi)^2} [\bar{\mathbf{X}}^{(2)}(\mathbf{p}|\mathbf{p}_1|\mathbf{p}_0)]^{aT} h(\mathbf{p} - \mathbf{p}_1) h(\mathbf{p}_1 - \mathbf{p}_0) \\ &= \int \frac{d^2\mathbf{p}_1}{(2\pi)^2} \bar{\mathbf{X}}^{(2)}(-\mathbf{p}_0|-\mathbf{p}_1|-\mathbf{p}) h(\mathbf{p} - \mathbf{p}_1) h(\mathbf{p}_1 - \mathbf{p}_0). \end{aligned} \quad (\text{B17})$$

From this we cannot deduce a result similar to Eq. (B16) for  $\bar{\mathbf{X}}^{(2)}$ . This fact is well illustrated with the following identity (which can be demonstrated with a transformation of the integration variables):

$$\int \frac{d^2\mathbf{p}_1}{(2\pi)^2} (\mathbf{p} + \mathbf{p}_0 - 2\mathbf{p}_1) h(\mathbf{p} - \mathbf{p}_1) h(\mathbf{p}_1 - \mathbf{p}_0) = 0. \quad (\text{B18})$$

We see that  $\mathbf{p}_1 \rightarrow \mathbf{p} + \mathbf{p}_0 - 2\mathbf{p}_1$  is not a null function, although

the integral is null. From this we deduce that  $\bar{\mathbf{X}}^{(n)}$  for  $n > 1$  is not unique. Moreover in using Eq. (B18) we can transform  $\bar{\mathbf{X}}^{(n)}$  in a reciprocal form. This procedure is illustrated in the one-dimensional case in Ref. 21, and the results for the second-order in the electromagnetic case are given in Refs. 8 and 22.

\*Electronic address: soubret@cpt.univ-mrs.fr

- <sup>1</sup>F. G. Bass and I. M. Fuks, *Wave Scattering from Statistically Rough Surfaces* (Pergamon, Oxford, 1979).
- <sup>2</sup>A. Ishimaru, *Wave Propagation and Scattering in Random Media* (Academic, New York, 1978).
- <sup>3</sup>F. T. Ulaby, R. K. Moore, and A. K. Fung, *Microwave Remote Sensing* (Addison-Wesley, Reading, MA, 1986), Vol. 2.
- <sup>4</sup>L. Tsang, G. T. J. Kong, and R. Shin, *Theory of Microwave Remote Sensing* (Wiley-Interscience, New York, 1985).
- <sup>5</sup>J. A. DeSanto and G. S. Brown, in *Progress in Optics XXIII*, edited by E. Wolf (Elsevier, Amsterdam, 1986).
- <sup>6</sup>J. A. Ogilvy, *Theory of Wave Scattering From Random Rough Surfaces* (Hilger, Bristol, 1991).
- <sup>7</sup>S. M. Rytov, Y. A. Kravtsov, and V. I. Tatarskii, *Principle of Statistical Radiophysics* (Springer-Verlag, Berlin, 1989), Vols. 3 and 4.
- <sup>8</sup>A. G. Voronovich, *Wave Scattering from Rough Surfaces* (Springer, Berlin, 1994).
- <sup>9</sup>A. K. Fung, *Microwave Scattering and Emission Models and their Applications* (Artech, Boston, 1994).
- <sup>10</sup>M. Nieto-Verperinas, *Scattering and Diffraction in Physical Optics* (Wiley, New York, 1991).
- <sup>11</sup>V. Freilikher, E. Kanziemper, and A. A. Maradudin, *Phys. Rep.* **288**, 127 (1997).
- <sup>12</sup>S. O. Rice, *Commun. Pure Appl. Math.* **4**, 351 (1951).
- <sup>13</sup>J. T. Johnson, *J. Opt. Soc. Am. A* **16**, 2720 (1999); **17**, 1685(E) (2000).
- <sup>14</sup>I. M. Fuks and A. G. Voronovich, *Waves Random Media* **10**, 253 (2000).
- <sup>15</sup>A. G. Voronovich, *Waves Random Media* **4**, 337 (1994).
- <sup>16</sup>G. C. Brown, V. Celli, M. Haller, and A. Marvin, *Surf. Sci.* **136**, 381 (1984).
- <sup>17</sup>A. R. McGurn, A. A. Maradudin, and V. Celli, *Phys. Rev. B* **31**, 4866 (1985).
- <sup>18</sup>V. Celli, A. A. Maradudin, A. M. Marvin, and A. R. McGurn, *J. Opt. Soc. Am. A* **2**, 2225 (1985).
- <sup>19</sup>A. R. McGurn and A. A. Maradudin, *J. Opt. Soc. Am. B* **4**, 910 (1987).
- <sup>20</sup>C. Baylard, J. J. Greffet, and A. A. Maradudin, *J. Opt. Soc. Am. A* **10**, 2637 (1993).
- <sup>21</sup>A. A. Maradudin and E. R. Méndez, *Appl. Opt.* **32**, 3335 (1993).
- <sup>22</sup>A. R. McGurn and A. A. Maradudin, *Waves Random Media* **6**, 251 (1996).
- <sup>23</sup>J. A. Sánchez-Gil, A. A. Maradudin, J. Q. Lu, V. D. Freilikher, M. Pustilnik, and I. Yurkevich, *Phys. Rev. B* **50**, 15 353 (1994).
- <sup>24</sup>However, we have to mention the work Ref. 32, where they considered a two-dimensional film. Their method, in principle, has the same domain of validity as the SPM; the difference comes from their use of a sophisticated development called Wiener-Hermite expansion to write down the scattered fields.
- <sup>25</sup>J. J. Greffet, *Phys. Rev. B* **37**, 6436 (1988).
- <sup>26</sup>G. S. Brown, *Wave Motion* **7**, 195 (1985).
- <sup>27</sup>M. Nieto-Verperinas, *J. Opt. Soc. Am. A* **72**, 539 (1982).
- <sup>28</sup>We use the same symbol for a function and its Fourier transform; they are differentiated by their arguments.
- <sup>29</sup>We explicitly show the permittivity dependence of  $\bar{\mathbf{R}}_s$ , with the subscript  $\epsilon_0, \epsilon_1$ , because we use an  $\bar{\mathbf{R}}_s$  matrix with different permittivity values.
- <sup>30</sup>Throughout this paper, the symbol  $H$  in the upper index is related to the height of a surface, and in the lower index to the polarization.
- <sup>31</sup>A. Ishimaru, C. Le, Y. Kuga, L. A. Sengers, and T. K. Chan, *PIER* **14**, 1 (1996).
- <sup>32</sup>T. Kawanishi, H. Ogura, and Z. L. Wang, *Waves Random Media* **7**, 35 (1997).
- <sup>33</sup>J. Q. Lu, J. A. Sánchez-Gil, E. R. Méndez, Z. Gu, and A. A. Maradudin, *J. Opt. Soc. Am. A* **15**, 185 (1998).
- <sup>34</sup>Y. S. Kaganovskii, V. D. Freilikher, E. Kanziemper, Y. Nafcha, M. Rosenbluh, and I. M. Fuks, *J. Opt. Soc. Am. A* **16**, 331 (1999).
- <sup>35</sup>J. A. Sánchez-Gil, A. A. Maradudin, J. Q. Lu, V. D. Freilikher, M. Pustilnik, and I. Yurkevich, *J. Mod. Opt.* **43**, 435 (1996).
- <sup>36</sup>A. Soubret, G. Berginc and C. Bourrely, cond-mat/0101373 (unpublished).